

**EFFECT OF THICKNESS GRADIENT ON CREEP
BEHAVIOUR IN A ROTATING COMPOSITE DISC**

*A dissertation report submitted in the partial fulfillment of the requirements for the award of
degree of*

Master of Engineering
IN
CAD/CAM & ROBOTICS

Submitted by
JASKARAN SINGH
Roll No: 801181017

Under The Guidance of
Mr. KISHORE KHANNA
(Assistant Professor)



**DEPARTMENT OF MECHANICAL ENGINEERING
THAPAR UNIVERSITY, PATIALA – 147004
JULY 2013**

DECLARATION

I hereby declare that the dissertation entitled “EFFECT OF THICKNESS GRADIENT ON CREEP BEHAVIOUR IN A ROTATING COMPOSITE DISC” is an authentic record of my study carried out as partial fulfilment for the award of the degree of **Master of Engineering in CAD/CAM & Robotics** at **Thapar University, Patiala** under the guidance of Mr Kishore Khanna, Assistant Professor, Department of Mechanical Engineering, Thapar University, Patiala in July 2013. The matter in this report has not been submitted in part or full to any other university or any institution for the award of any other degree.


(Jaskaran Singh)

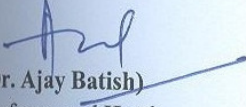
Reg. No. 801181017


This is to certify that above declaration made by the student concerned is correct and to the best of my knowledge and belief.


(Kishore Khanna)
(Assistant Professor)

Department of Mechanical Engineering,
Thapar University, Patiala – 147004

Countersigned by:


(Dr. Ajay Batish)
Professor and Head,
Department of Mechanical Engineering
Thapar University, Patiala – 147004


(Dr. S.K. Mohapatra)
Sr. Professor &
Dean of Academic Affairs,

ACKNOWLEDGEMENT

I am highly grateful to the authorities of Thapar University, Patiala for providing this opportunity to carry out the dissertation work. I would like to express a deep sense of gratitude and thank profusely to my guide Mr. Kishore Khanna for his sincere and invaluable guidance, suggestions and attitude which inspired me to submit this report in the present form.

I am also thankful to other faculty members of Mechanical Engineering Department, TU, Patiala for their intellectual support.

My special thanks are due to my family members and friends who constantly encouraged me to complete this work.

(Jaskaran Singh)

ABSTRACT

The creep behaviour of a rotating disc having variable thickness and made of isotropic aluminium-silicon carbide particulate composite has been investigated. The stress and strain rates in the disc have been obtained by using threshold stress based creep law. A computer code based on the mathematical analysis is developed to obtain creep response of rotating composite disc. Different thickness profiles have been considered to investigate their effect on stresses and strains are compared. The effects of changing the particle size of reinforcement have also been investigated.

TABLE OF CONTENTS

Sr. No.	TITLE	PAGE No.
	DECLARATION	
	ACKNOWLEDGEMENT	i.
	ABSTRACT	ii.
	TABLE OF CONTENTS	iii.
	LIST OF FIGURES	vi.
	CHAPTER 1: INTRODUCTION	1-20
1.1	Composite Materials	1
1.2	History of Composites	2
1.3	Mechanical Advantages of Composite Materials	3
1.4	Parameters for Selection of Composites	4
1.5	Factors Affecting Mechanical Performance	4
1.6	Types of Composites	7
1.7	Classification of Composite Materials	8
1.8	Properties of Aluminium Based MMCs	13
1.9	Advantages of using Composites over Conventional Materials	14
1.10	Applications of Composite Materials	15
1.11	Limitation of Composites	16
1.12	Creep	17
1.13	Rotating Disc	19
1.14	Applications of Rotating Disc	20
	CHAPTER 2: LITERATURE REVIEW	21-29
	CHAPTER 3: PROBLEM FORMULATION	30-31
3.1	Gaps in the Literature	30
3.2	Purposed Work	30
3.3	Methodology	31

CHAPTER 4: MATHEMATICAL ANALYSIS OF CREEP	32-43
4.1 Assumptions	32
4.2 Maximum Shear Stress Criterion (Tresca Yield Criterion)	33
4.3 Analysis of Creep	34
4.4 Equilibrium Equation for Rotating Disc	37
4.5 Disc Profile	41
4.6 Calculation of Area and Inertia of Discs	42
4.7 Solution Procedure	42
CHAPTER 5: RESULTS AND DISCUSSIONS	44-56
5.1 Validation	44
5.2 Effect of Disc Profile on Creep Behaviour of Disc	46
5.3 Effect of Varying Particle Size on Creep Behaviour of Disc	52
CHAPTER 6: CONCLUSIONS	57
FUTURE SCOPE OF WORK	58
REFERENCES	59-63

LIST OF FIGURES

Fig. No.	Name of Figure	Page No.
Fig 1.1	Thin slabs in plywood	2
Fig 1.2	Specific strength as a function of time of use of materials	3
Fig 1.3	(a) Short fiber composite (b) Long fiber composites	5
Fig 1.4	Natural composites	7
Fig 1.5	Synthetic composites	8
Fig 1.6	Classification of composite materials	8
Fig 1.7	Continuous fiber composites	9
Fig 1.8	Discontinuous fiber composites	10
Fig 1.9	Schematic representation of particulate composites	11
Fig 1.10	Application of composites in various sectors	16
Fig 1.11	Creep curve showing the three stages of creep	18
Fig 1.12	Rotating disc	19
Fig 4.1	Free body diagram of an element of the disc	37
Fig 4.2	Numerical scheme of computation	43
Fig 5.1	Comparison of radial stress for present study with published result	46
Fig 5.2	Effect of disc thickness on radial stress	47
Fig 5.3	Effect of disc thickness on tangential stress	48
Fig 5.4	Effect of disc thickness on tangential strain rate	49
Fig 5.5	Effect of disc thickness on radial strain rate	50
Fig 5.6	Effect of disc thickness on axial strain rate	51
Fig 5.7	Effect of varying the particle size on radial stress	52
Fig 5.8	Effect of varying the particle size on tangential stress	53
Fig 5.9	Effect of varying the particle size on tangential strain rate	54
Fig 5.10	Effect of varying the particle size on radial strain rate	55
Fig 5.11	Effect of varying the particle size on axial strain rate	56

INTRODUCTION

1.1 Composite Material

A composite is a structural material that consists of two or more combined constituents that are combined at microscopic level and are not soluble in each other. One constituent is called reinforcement phase and one in which it is embedded is called the matrix. The reinforcement phase may be in the form of fibres, particles, or flakes. The matrix phase materials are generally continuous.

A composite material can provide superior and unique mechanical and physical properties because it combines the most desirable properties of its constituents while suppressing their least desirable properties. The composite materials possess characteristic properties, such as high stiffness, great strength, low weight, high temperature performance, good corrosion resistance, great hardness and conductivity that are not possible in any of its constituents alone. Examination of these properties reveals that they depend on the following [31]

- Properties of the individual constituents.
- Relative amounts of the constituents.
- Size and shape of the constituents (i.e. Morphology).
- Degree of bonding between constituents.
- Orientation of the various constituents.

Traditional engineering materials (steel, aluminium etc.) contain impurities that can represent different phases of the same material and the broad definition of a composite, but are not taken as a composite because the elastic modulus or strength of the impurity phase is nearly identical to that of the pure material. The meaning of a composite material is flexible and can be improved to fit specific requirements.

1.2 History of Composites

One of the earliest known composite materials is adobe brick in which straw (a fibrous material) is mixed with mud or clay (an adhesive with strong compressive strength). The straw allows the water in the clay to evaporate and distribute cracks in the clay uniformly, greatly improving the power of this early construction material. Alternative form of a composite material is the ubiquitous construction material called plywood. Plywood (Fig1.1) uses natural materials (thin slabs of wood) held together by a tough adhesive, creating the structure solidier than just the wood. In nature, wicker is also a example of a wood composite structure, combining a cellulose fiber and lignin, through the lignin give the adhesive to hold the fibers together. [32]



Fig 1.1: Thin slabs in plywood.[31]

Reinforced concrete is a combination of two remarkable materials, concrete (a composite by itself) and steel that takes advantage of the strengths of each material to overcome their distinct limitations in each. Steel has very high tensile strength, but concrete has very high compressive strength. In combination, they make a greater material for road and bridge construction.

Today, when we speak of composite materials, or just ‘composites’, we are referring to the highly engineered combinations of polymer resins and reinforcing materials such as glass fibers. A fibreglass composite structure is a combination of glass fibers of various lengths and resins such as vinyl ester or polyester. The term FRP is frequently used, sense Fiber Reinforced Plastic. FRP is a very common term for many different combinations of reinforcement materials and bonding resins. Thus, the term “composites” is used extremely broadly to describe many materials with many different properties targeted at an even larger

number of applications. To show how composites have improved our world, look no more than under the hood of a modern car and realize that most of what we can see are components made of composite materials.

1.3 Mechanical Advantages of Composite Materials

Next two parameters are generally used to measure the relative advantages derived from composite materials.[29]

(a) Specific modulus

(b) Specific strength

Specific modulus is defined as the ratio of Young's Modulus (E) and density (ρ) of the materials.

$$\text{Specific modulus} = E/\rho$$

Specific strength is defined as ratio between strength and density of the materials.

$$\text{Specific strength} = \sigma/\rho$$

The two ratios are high in composite materials. For example, the power of a graphite/epoxy unidirectional composite material is same as that of steel but specific strength of this composite is three times that of steel thereby saving in cost of material and energy. Fig 1.2 shows how composites and fiber rate with other traditional materials in terms of specific strength. [29]

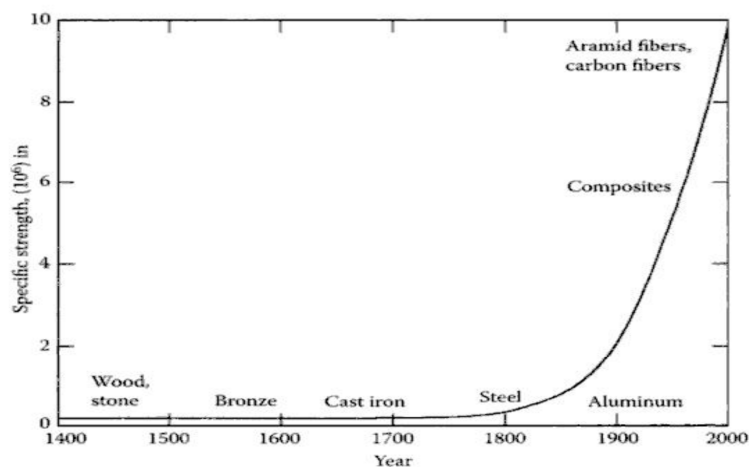


Fig 1.2: Specific strength as a function of time of use of materials. [29]

1.4 Parameters for Selection of Composites

For selecting a composite material for a particular application, the following six parameters are to be considered: [31]

- i) Strength
- ii) Toughness
- iii) Formidability
- iv) Join ability
- v) Corrosion
- vi) Wear Resistance
- vii) Affordability.

1.5 Factors Affecting Mechanical Performance

The mechanical enactment of composite materials depends on number of factors such as [31]:

I. Fiber Factor

II. Matrix Factor

III. Other Factors (Fiber matrix interface, etc.)

I. Fiber factor: It involves the following four parameters.

- a) Length
- b) Orientation
- c) Shape
- d) Material

a) **Length :** Fiber can be either short or long in the length as shown in Fig 1.3



Fig 1.3 (a) Short fiber composite (b) Long fiber composite [31]

Long continuous fibers are easy to orient and process while short fibers cannot be fully controlled or oriented properly. More, long fibers provide several benefits over short fibers including high impact resistance, little shrinkage, better surface finish and dimensional stability. On the other hand, short fibers deliver low cost, easy to work with and have fast cycle time fabrication procedures. Short fibers have few flaws, therefore leading to higher strength.

b) Orientation: The distribution of fiber in a matrix can be random or aligned in a specific direction to achieve very high stiffness and strength in that path. If fibers are oriented in more than one way in matrix, the composite will display possess high stiffness and strength along these directions.

c) Shape: The most common shape of fibers is circular because of ease of handling and manufacturing. Hexagonal and square-shaped fibers are probable but their advantages of strength and high packing factors do not outweigh the difficulty in handling and processing.

d) Material: The material of fiber directly influences the mechanical performance of a composite. Fibers are commonly expected to have high elastic modulus and strength. This hope along with the low cost are the key factors that graphite, aramids and glass fibers lead the fiber market for composites.

II. Matrix Factors

Fibers are used as reinforcement to matrix. The matrix functions contain binding of the fibers together, shielding fibers from environment, protecting from damage during handling and load transfer from matrix to fibers. In general, the matrix holds sub standard properties compared fibers.

III. Other Factors

A part from fiber and matrix there are several other factors which can affect the mechanical performance of composite materials. The fiber-matrix interface is a vital factor which determines how well the matrix transfers the loads to the fibers.

The fiber-matrix interfacial relationship is of following three types:

- a) Chemical Bonding
- b) Mechanical Bonding
- c) Reaction Bonding

a) Chemical Bonding

Chemical bonding is formed between the fiber surface and the matrix. Some fibers bond obviously to the matrix while others do not. Coupling agents are frequently added to form a chemical bond.

b) Mechanical Bonding

Natural roughness and etching of the fiber surface causing interlocking may form a mechanical bond between the fiber and the matrix. If the factor of thermal expansion of the matrix is higher than that of fiber, and the manufacturing temperatures are greater than the operating temperatures, the matrix will shrink extra than the fiber, initiating the compression of matrix around the fiber.

c) Reaction Bonding

Reaction bonding occurs when atom or molecules of fiber and matrix diffuse into each other at interface. This inter diffusion often generates a distinct interfacial layer, which has dissimilar properties than that of fiber or matrix. Though, this thin layer aids to form a bond

but it also forms micro cracks in the fiber. These micro-cracks decrease the strength of fiber which ultimately leads to poor strength of composite materials.

1.6 Types of Composites

Composites are divided into mainly two types:

- i) Natural Composites (existing in nature)
- ii) Synthetic Composites (man-made)

Natural Composites:

Wood is an interesting example of natural composites. The longitudinal hollow cells of wood are made up of layers of spirally wound cellulose fibers with varying spiral angle bounded together with lignin during the growth of tree.



Fig 1.4: Natural composites

Bone is also a composite material composed primarily of organic fibers, small inorganic crystals, water and fats.

Synthetic Composites:

The automotive industry presented large-scale use of synthetic composites.



Fig 1.5: Composites used in automobiles (Synthetic composites)

1.7 Classification of Composite Materials:

Composites are classified by the geometry of the reinforcement as particulate, flake and fiber or by the type of matrix as polymer, metal, ceramic and carbon as shown in Fig.1.6

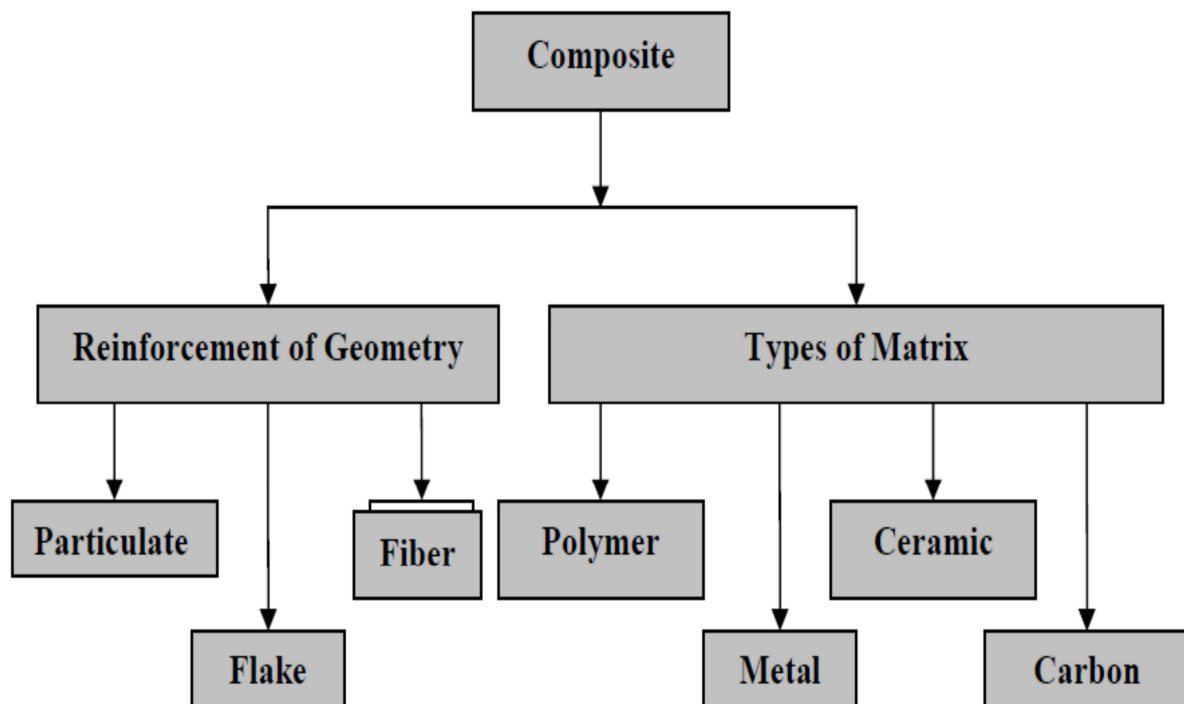


Fig 1.6: Classification of composite materials [31]

1. Classification Based on Geometry of Reinforcement

Two broad classes of composites are:

- a) Fiber
- b) Particulate

Each has distinctive properties and application potential, and can be subdivided into specific categories as discussed below.

Fiber:

A fibrous composite consists of either continuous (long) or chopped (whiskers) fibers suspended in a matrix material. Equally continuous fibers and whiskers can be identified from a geometric viewpoint:

a) Continuous Fibers:

A continuous fiber is geometrically characterized as having a very high length - to - diameter ratio. They are normally stronger and stiffer than bulk material. Continuous fiber composites can be either single layer or multilayered. The single layer continuous fiber composites can be either unidirectional or woven, and multilayered composites are commonly referred to as laminates. The material response of continuous fiber composite is generally orthotropic. Schematics of Fiber diameters generally range between 0.00012 and 0.0074 μin (3-200 μm) depending upon the fiber.

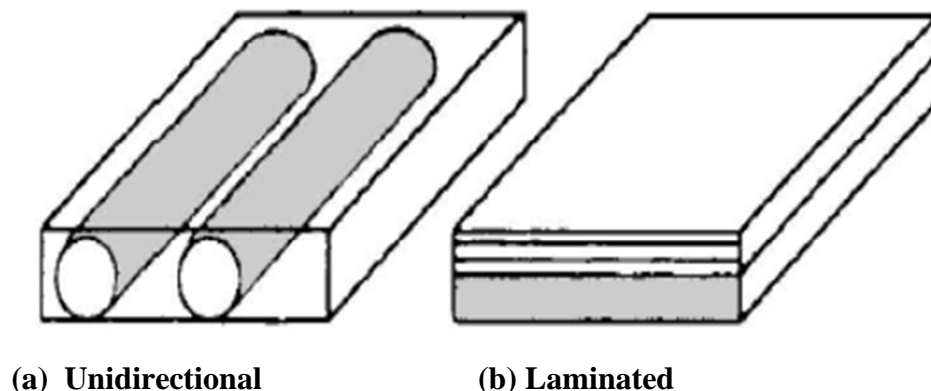
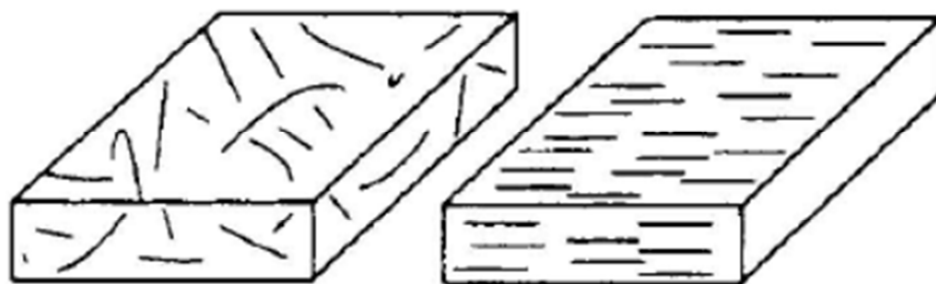


Fig 1.7: Continuous fiber composites [32]

b) Whiskers:

A whisker is generally considered to be a short, stubby fiber. Composites in which the reinforcements are discontinuous fibers or whiskers can be produced so that the reinforcements have random orientation. Material systems made of discontinuous reinforcements are considered single layer composites. It can be broadly defined as having a length – to - diameter ratio of $5 < l/d < 1000$ and beyond. Whisker diameters generally range between $0.787 \mu\text{in}$ and $3937 \mu\text{in}$ ($0.02 - 100 \mu\text{m}$). The discontinuities can produce a material response that is anisotropic, but in many instances the random reinforcements produce nearly isotropic composites.



(a) Random fiber orientation (b) Biased fiber orientation

Fig 1.8: Discontinuous fiber composites [32]

Particulate:

A particulate composite is characterized as being composed of particles suspended in a matrix. Particles can have practically any shape, size or configuration. Examples of well - known particulate composites are concrete and particle board. There are two subclasses of particulates:

- a) Flake and
- b) Filled/skeletal:

a) Flake.

A flake composite is normally composed of flakes with large ratios of platform area to thickness, suspended in a matrix material (particle board, for example).

b) Filled/Skeletal.

A filled/skeletal composite is composed of a continuous skeletal matrix filled by a second Material. For example, a honeycomb core filled with an insulating material. The response of a particulate composite can be either anisotropic or orthotropic. Such composites are used for many applications in which strength is not a significant component of the design. A diagram of several types of particulate composites is shown in Figure 1.9

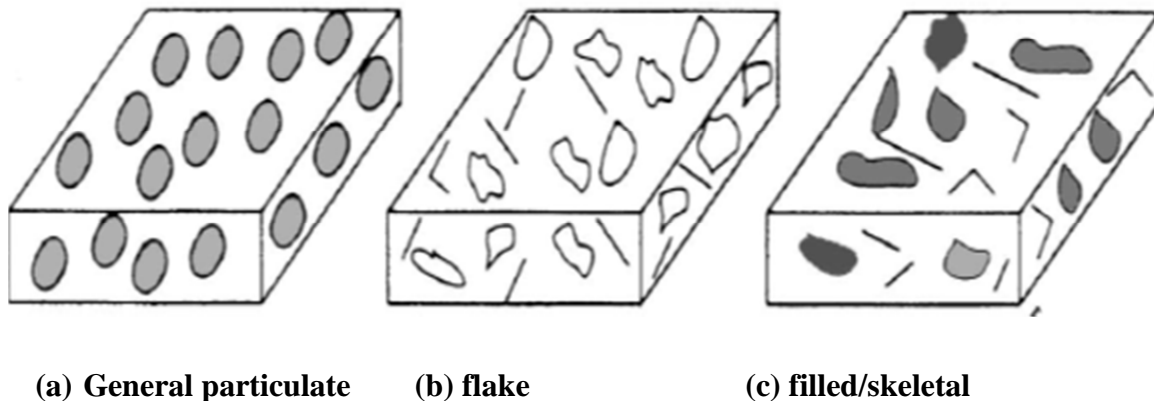


Fig 1.9: Schematic representation of particulate composites. [32]

2. Classification Based on Matrix

Based on the type of matrix, Composites are of the following types [31]:

- (a) Polymer Matrix Composite (PMC)
- (b) Metal Matrix Composite (MMC)
- (c) Ceramic Matrix Composite (CMC)
- (d) Carbon –Carbon Composite

(a) Polymer Matrix Composite (PMC)

Polymer matrix composites are the most advanced composites. These composites consist of a polymer (e.g., epoxy, polyester, urethane etc) reinforced by thin-diameter fibers (for example: - graphite, aramids, boron etc). These are commonly employed due to their little cost, great strength and simple manufacturing principle. As an example, graphite/ epoxy composites are approximately five times stronger than steel on a weight-for-weight basis. Main drawback of Polymer Matrix Composites (PMCs) include low operational temperature, great coefficient of thermal and moisture expansion and low elastic properties in certain

directions. However, the advantages include its strength, low cost, high chemical resistance and good insulating property.

(b) Metal Matrix Composite (MMC)

This class of composite materials consists of metallic matrix which is usually ductile. The ductile matrix can be aluminium, copper, magnesium, titanium, nickel, super alloy or even an inter metallic compound. The reinforcing fibers may be graphite, boron carbide, alumina or silicon carbide. Fine whiskers of cobalt, silicon carbide, silicon nitride, leads of titanium, tungsten, molybdenum, beryllium and stainless steel etc have also been used as reinforcement.

Compared to conventional engineering materials, these composites offer higher stiffness and strength, specifically at elevated temperatures, small coefficient of thermal expansion and enhanced resistance to fatigue, abrasion and wear. Matched to organic matrix materials, they offer great heat resistance and better electrical and thermal conductivity.

Graphite-reinforced aluminium can be designed to have near zero thermal expansion in the fiber direction. Aluminium oxide-reinforced aluminium matrix composites have been extensively used in automotive connecting rods to provide high stiffness with low weight. Aluminium reinforced with silicon carbide whiskers has been fabricated into aircraft wing panels, providing 20-40% weight saving. Fiber reinforced super alloy has potential future for applications such as turbine blades.

(c) Ceramic Matrix Composite (CMC)

Ceramic matrix composites possess properties like high melting points and great corrosion resistance, stability at elevated temperatures and high compressive strength. These types of materials can even be used at very high temperatures (i.e. above 1500°C).

(d) Carbon –Carbon Composite

These composites retain their properties even at exceptionally very high temperatures in the range of 3315°C. Their dimensional stability is also good and therefore can be used at elevated temperatures. They are 20 times stronger and 30% lighter than the Graphite fibers. Carbon by itself is brittle and flaw sensitive like the ceramics. Reinforcement of the carbon matrix allows the composite to fail gradually and also gives advantages such as ability to

withstand high temperatures, low creep at high temperatures, small density, respectable tensile and compressive strengths, great fatigue resistance, great thermal conductivity and high coefficient of friction.

3. Aluminium /Aluminium Alloy Based MMCs

MMCs based on aluminium and its alloys are widely used in engineering and structural applications due to their low weight, which is the primary condition in most of the MMC's applications. In addition to this, aluminium/aluminium alloy based MMCs are economical compared to other light metals, like as titanium and magnesium. The brilliant strength, ductility and corrosion resistance of MMCs are well established and can be modified to fulfil the requirement of different applications ranging from automotive and aircraft industry to sports and leisure. The development work related to aluminium/aluminium alloy matrix composites is currently focused on following two sectors [32]:

- i) Continuous fiber reinforced composite with greater properties for every specific applications.
- ii) Mass production technologies of low-cost discontinuously reinforced composites with moderate properties for wider range of applications.

1.8 Properties of Aluminium Based MMCs:

The noticeable properties of aluminium based MMCs are [31]:

- a) Specific Stiffness
- b) Specific Strength
- c) Fatigue Resistance
- d) Coefficient of Thermal Expansion
- e) Wear Resistance

a) Specific Stiffness

The addition of stiff metallic or ceramic reinforcement materials to the metal matrix results in an increase in elastic modulus of the composites materials. In event of light weight metals, like aluminium, titanium and magnesium, the rise can be very important even at moderate levels of reinforcement addition.

b) Specific Strength

In addition to high stiffness, aluminium based MMCs also possess high strength. The strength of the composite is powerfully dependent on the specific characteristics of the reinforcement material, its morphology and the nature of bonding at reinforcement-matrix interface. Continuous fiber reinforced composites display high specific strength levels in the direction of the fiber orientation.

c) Fatigue Resistance

The addition of reinforcement in aluminium/aluminium alloy matrix significantly affects its fatigue resistance. The mechanisms of fatigue resistance improvement differ in composites depending on the morphology of the reinforcement and characteristics of reinforcement-matrix interface.

d) Coefficient of Thermal Expansion (CTE)

The distinctive ceramic reinforcements for MMCs have significantly lower values of the coefficient of thermal expansion (CTE) than the metal matrix into which they are incorporated. Thus, the addition of ceramic reinforcement to the high expansion metals such as aluminium, magnesium, copper, and titanium can effect in substantial reduction in the CTE.

e) Wear Resistance

The high hardness of the typical ceramic reinforcement materials can also affect the tribological properties of the metal matrix composites compared to pure matrix. Particulate reinforced MMCs for particular interest for use in wear resistance dominated applications.

1.9 Advantages of Using Composites over Conventional Materials [31]

- i) Very high specific strength. This means very high strength and low weight.
- ii) Great freedom of shape. Double curved and complex parts can be simple produced.
- iii) High degree of integration possible. Which means simple combination of stiffeners, inserts, cores, and creation of self supporting structures in one or two production cycles?

- iv) Excellent fatigue endurance concerning number of load cycles(many time higher than with metals) and residual fatigue strength (aramide and carbon epoxy laminates retain more than 60% of their residual static strength, which is advanced than is possible with metals.)
- v) Material can be tailored. This means fit for the loads/performance the end product has to perform during its life time.
- vi) Brilliant chemical resistance against acids, chemical etc.
- vii) Brilliant weather/water resistance. Material has almost no corrosion takes no little water which leads to low maintenance cost especially on long run.
- viii) Composites have excellent RAM features (Radar absorbing material). It's also possible to make special laminates which are radar and sonar transparent.
- ix) Excellent impact habits.
- x) Excellent electrical habits, concerning isolation but also conduction, dialectical habits, EMS shielding etc. Structure can be tailored on RF transparency but can also be made RF reflecting.
- xi) Countless thermal isolation practises, fire retardant habits, and high temperature performance.

1.10 Applications of Composites:

- i) Automobile
- ii) Marine
- iii) Aerospace
- iv) Construction
- v) Electrical
- vi) Sporting goods
- vii) Medical

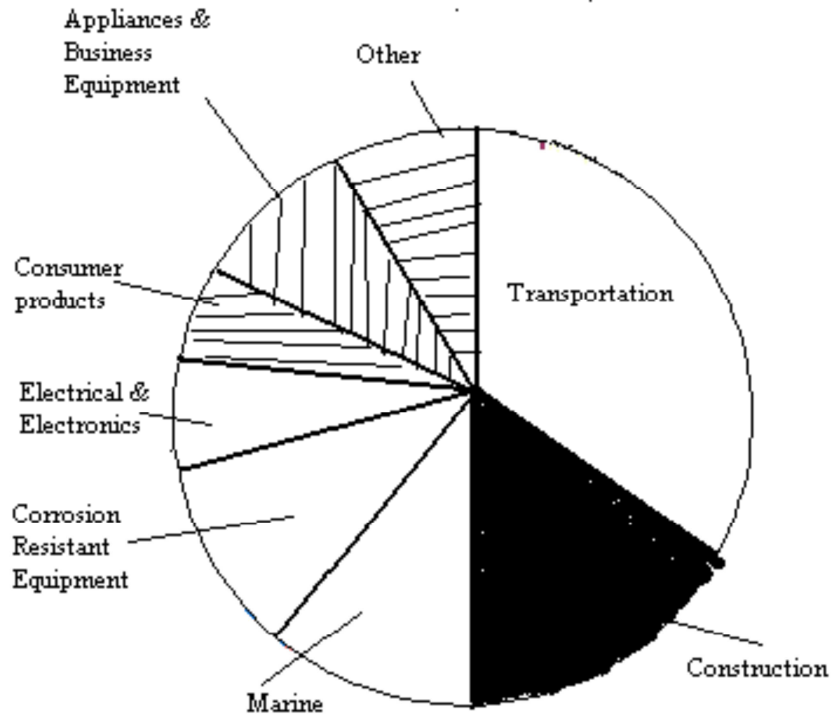


Fig 1.10: Application of composites in various sectors [29]

1.11 Limitation of Composites [32]

Besides having so many advantages composite material have some limitations:

- a) High cost of fabrication of composite materials. For example, a portion made-up of graphite/epoxy composite may cost up to 10 to 15 times of materials cost.
- b) Mechanical characterization of composite structure is more complex than that of a metal structure. Composite materials remain not isotropic (i.e. do not possess same properties in all the direction). For example, a distinct layer of graphite/epoxy composite requires nine stiffness and strength constants for conducting mechanical analysis while in the case of steel only four stiffness and strength constant are required.
- c) Repair of composite is not a simple process as compared to metals. Composites do not have good combination of strength and fracture toughness as compared to metals.

1.12 Creep

The progressive deformation of a material at constant load is called creep. The degree of this deformation is a meaning of the material properties, exposure time, experience temperature and the applied structural load. Dependent on the amount of the applied stress and its period, the deformation may develop so large that a component can no longer perform its job, for example creep of a turbine blade will cause the blade to contact the casing, causing in the failure of the blade. Creep is commonly of concern to engineers and metallurgists when evaluating components that operate under high stresses or high temperatures. Creep is a distortion mechanism that may or may not constitute a disaster mode. Moderate creep in concrete is occasionally welcomed because it relieves tensile stresses that might otherwise lead to cracking. [31]

Unlike brittle fracture, creep deformation does not occur suddenly upon the presentation of stress. Instead, strain accrues as a result of long-term stress. Creep is a "time-dependent" deformation.

The temperature range in which creep deformation may occur differs in various materials. For example, tungsten needs a temperature in the thousands of degrees before creep deformation can occur while ice will creep near 0 °C (32 °F). As a rule of thumb, the effects of creep deformation generally become noticeable at approximately 30% of the melting point (as measured on a thermodynamic temperature scale such as Kelvin or Rankin) for metals and 40–50% of melting point for ceramics. Effectively any material will creep upon approaching its melting temperature. Since the slightest temperature is relative to melting point, creep can be seen at reasonably low temperatures for selected materials. Plastics and low-melting-temperature metals, containing many solders, creep at room temperature as can be seen markedly in old lead hot-water pipes. Glacier flow is an example of creep practises in ice.

To determine the engineering creep curve of a metal, a constant load is practical to a tensile specimen maintained at a constant temperature and the strain (extension) is determined as a meaning of time. Curve A in the Fig 1.11 explains the ideal shape of the creep curve. The gradient of this curve ($d\varepsilon/dt$) is referred to as the creep rate. A typical creep curve exhibits three stages which are readily distinguishable and depend strongly on the applied stress and temperature. The first stage of the creep, known as primary creep, represents a region of declining creep rate. Primary creep is a period of predominantly

transient creep in which the resistance of the material increases by virtue of its own deformation. Primary creep occurs at small temperature and low stress levels.[31]

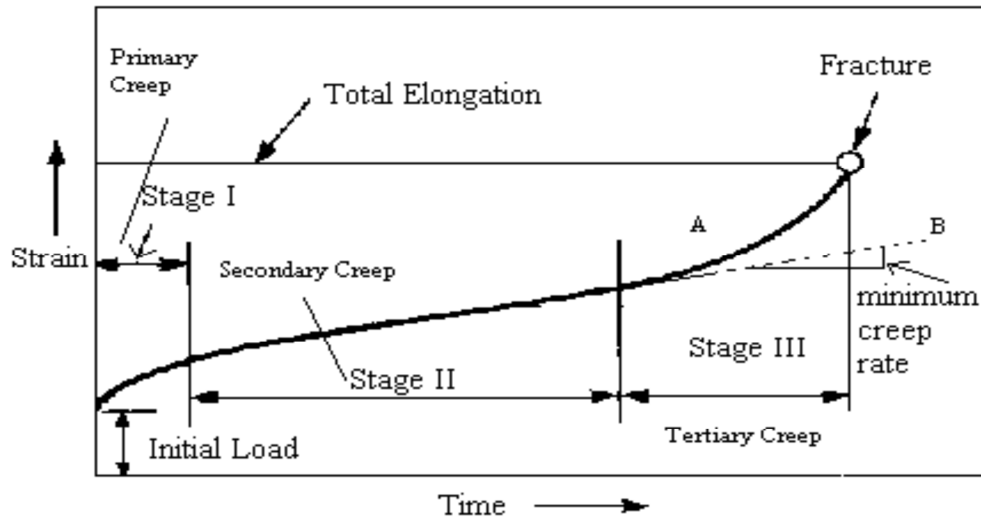


Fig1.11: Creep curve showing the three stages of creep. [31]

(Curve A- Constant load curve, Curve B- Constant stress test).

The second stage of creep, known also as secondary creep, is a period of closely constant creep rate which result from a balance between the competing processes of strain hardening and recovery. For this cause, secondary creep is generally referred to as Steady State Creep. The middling value of the creep rate during secondary creep is called the minimum creep rate.

Third stage or tertiary creep primarily happens in constant load creep tests at high stresses and high temperature. Tertiary creep happens when there is an actual reduction in cross-sectional area either because of necking or internal void formation. Third stage creep is frequently related with metallurgical changes such as coarsening of precipitate particles, recrystallization or diffusion changes in the phases present. The dashed line (Curve B) in Fig1.11 shows the shape shows the shape of a constant-stress creep curve. In engineering situations, it is usually the load, not the stress that is maintained constant, so a constant load creep test is more important .[31]

1.13 Rotating Disc

Rotating disc [27] is an early invention during progress of civilization and provides an area of research and studies intensively pursued due to their vast utilization in rotating machinery namely turbine rotors, compressors, flywheels, disc brakes of automobiles and gears, computer disc drives etc. Optimal and more reliable design of rotating discs has long been an important issue in engineering design since very long. By changing suitably the geometrical parameters and physical properties, the optimal and more reliable design of a rotating disc for given operating conditions (i.e. load, speed, operating temperature) can be achieved.

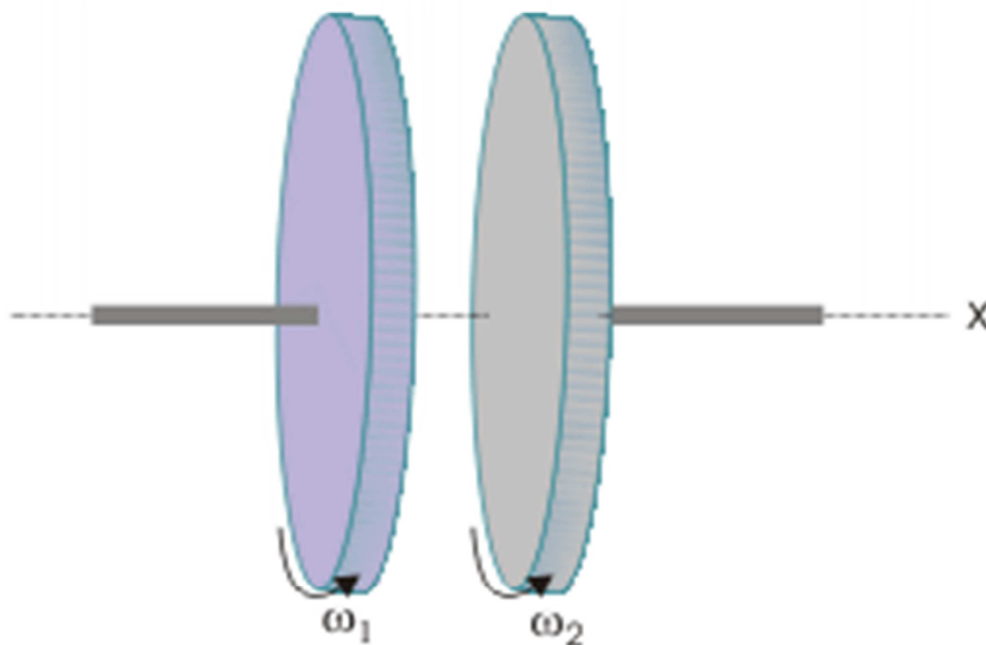


Fig 1.12: Rotating disc

Discs of gas turbines, jet engines and automotive and aerospace braking systems are usually operated at relatively higher angular speeds and subjected to high temperature/thermal gradient. Therefore, the estimate of long term steady state creeps deformations is very important for these applications. A reduced weight of such components, resultant from the use of aluminium / aluminium base alloys, is expected to save power and fuel due to a reduction in the payload. However, the enhanced creep of aluminium/aluminium alloys may not permit their use in such applications. Ceramic reinforced aluminium/aluminium matrix

composites have shown superior high temperature properties, therefore may be used for rotating disc applications exposed to elevated temperature.

1.14 Applications of Rotating Disc

- i) Turbine rotors
- ii) Compressors
- iii) Flywheels
- iv) Disc brakes of automobiles
- v) Gears
- vi) Computer disc drives

LITERATURE REVIEW

The review of literature carried out to accomplish this work is presented in the following section:

Jang *et al.* [15] prepared two types of functionally gradient materials (FGMs) by changing the spatial distribution of glass fiber (GF) and carbon fiber (CF) in polyphenylene sulphide (PPS) matrix. For measurement of the mechanical properties of FGMs and GF/CF/PPS isotropic composites, flexural and instrumented impact tests were done. The flexural strengths and the flexural modulus of GF/CF isotropic composites improved with the increment of CF relative volume ratio. On the other hand, total absorbed impact energy of GF/CF isotropic composites reduced with the addition of CF relative volume ratio. Matched with GF/CF isotropic composite, FGM G – to – C was display higher flexural strength and higher flexural modulus while FGM C–to–G signified similar values. From these results it was decided that the total impact absorption energies of the two FGMs were show a little increment compared with GF/CF isotropic composite and FGM fabrication with correct compositional gradient to achieve various or superior mechanical properties associated with the isotropic composite.

Lee *et al.* [21] applied centrifugal force in order to make a spatial gradient of fibre distribution in the epoxy/carbon fibre system. The gradient arrangement of the epoxy/carbon fibre composite was organized by changing the rotation time and the material factors, such as fibre length, fibre content and matrix viscosity. The spatial gradient dispersal of carbon fibres in an epoxy matrix was done by the combined mechanism of packing and settling. The mechanical possessions of the functionally gradient epoxy/carbon fibre composite were also examined and it was found that at the same extent of carbon fibre, the flexural power of the functionally gradient composite was greater than that of conventional isotropic composite.

Horgan *et al.* [7] expressed axisymmetric problem of a solid circular disk rotating around its central axis with a continuous angular velocity and traction-free on its surface. The body was composed of a linearly elastic inhomogeneous isotropic material with material properties that fluctuate only in the radial direction. An exact solution was achieved for a distinctive class of

inhomogeneous materials, namely those with a continuous Poisson's ratio and a Young's modulus with power-law requirement on the radial coordinate. They measured the case where the Young's modulus rises monotonically with radial distance from the centre, so that the power-law exponent n is positive. It was presented that the stress response of the inhomogeneous disk was considerably different from that of the homogeneous body. The maximum radial and hoop stresses were not happening at the centre as in the case for the homogeneous material. It was also exposed that for the general inhomogeneous isotropic case material inhomogeneity may be design so that the radial and hoop stress were same throughout the disk.

Ahmet *et al.* [1] obtained analytical solutions for the elastic–plastic stress distribution in rotating variable thickness annular disk under plane stress assumption. The thickness of the disk was supposed to vary in parabolic form in radial direction which pointers to hyper geometric differential equations for the solution. It was revealed that the plastic core advanced further by Tresca criterion than von Mises. Accordingly, von Mises criterion expected greater fully plastic limit angular velocities. It was also initiate that the maximum discrepancy between the two commonly used criteria was not more than 6% for the problems measured in this work.

Jahed *et al.* [13] presented a common axis-symmetric method by ranging the formerly suggested variable material properties (VMP) method for examination of primary and secondary creep in axis-symmetric problem of rotating discs and pressure vessels. The technique used the basic solution for a rotating constant isotropic disc and produced the solution for non-uniform inhomogeneous one. Primary and secondary creep performance was expected by the suggested method and the results were compared to FEM solutions.

Gupta *et al.* [27] investigated the steady state creep in a rotating disc made of isotropic aluminium–silicon carbide particulate composite. The creep behaviour of the composite was described by Sherby's constitutive model. The radial and tangential stresses and steady state creep rates in the disc were calculated and presented for various combinations of material parameters (like particle size and particle content) and temperatures. It was found that the tangential as well as radial strain rates in the disc reduced significantly with reducing particle size, with increasing particle content and with decreasing operating temperature. The study exposed that for given operating conditions, the strain rates in the disc can be controlled by selecting optimum particle content and/or particle size of the reinforcement.

Gupta et al. [28] analyzed the creep performance of a rotating disc with constant thickness made of isotropic functionally graded material (FGM). The disc under examination was made of composite containing silicon carbide particles in a matrix of pure aluminium. The creep behaviour was given by Sherby's law. The disc was supposed to hold thermal gradient in the radial direction. The study was indicated that for the linear particle distribution, the steady-state strain rates in FGM disc was suggestively lower compared that in an isotropic disc with uniform particle distribution. It was observed that the strain rates in composite discs operating under thermal gradient were reduced compared to similar discs under a uniform average temperature.

ERASLAN et al. [2] presented a parametric analysis of rotating variable thickness elastoplastic annular disks with inner boundaries exposed to pressure. A computer model based on von Mises yield criterion and nonlinear isotropic hardening was created. Elastic limit angular velocities, incompletely plastic deformations and plastic limit angular velocities were examined with emphasis on the purpose of the effects of all the geometric, material and hardening factors involved. The results obtained showed that in most cases the stresses, displacements and plastic strains, elastic and plastic limit angular velocities and width of the plastic region were affected meaningfully by the parameters used in the model.

Zenkour [5] presented correct elastic solutions for rotating annular disks. A new material possessions and density profile in exponential form having four geometric parameters was suggested. Analytical solutions using that profile were found in terms of Whittaker's functions for the elastic deformation of rotating annular disks. Special cases of rotating annular disks were examined, which include annular disks with constant thickness and constant density, exponentially variable elastic possessions and density, and exponentially profile graded disks. For all cases calculated, closed form solutions were found and numerical results were presented. The results involved the radial displacement, circumferential and radial stresses of the four annular disk configurations for combinations of homogeneous and exponentially graded cases. The pattenen of stresses and displacement were attained and evaluations between different cases were made at the same angular velocity.

Kordkheili et al. [23] applied a semi-analytical thermo elasticity solution for hollow and solid rotating axis-symmetric disks made of functionally graded materials. The radial domain was divided into some virtual sub-domains in which the power-law distribution was used for the thermo mechanical properties of the constituent components. Imposing the necessary

continuity conditions between adjacent sub-domains, together with the total boundary conditions, a set of linear algebraic equations were obtained. Solution of the linear algebraic equations yields the thermo elastic responses for each sub-domain as exponential functions of the radial coordinate. From the results, it was noted that the gradation of the constitutive components plays an important role in determining the thermo – mechanical response of FG rotating disk as well as in optimal design of this structure.

Bayat *et al.* [17] discussed that a variable thickness FG disc exposed to centrifugal body and thermal loading. Based on the form of the power-law distribution for the mechanical properties of the constituent components and the thickness profile function, the effects of the material grading index and the geometry of the disk on the stresses and displacements were studied. It was found that a functionally graded rotating disk with parabolic or hyperbolic convergent thickness profile has smaller stresses and displacements compared with that of uniform thickness. Also for the same grading index, n , concave thickness profile was the lightest disk than the linear and convex, whereas uniform thickness provided the heaviest disc.

Deepak *et al.* [8] explained the effect of the stress exponent on the steady state creep in a rotating disc made of isotropic aluminium–silicon carbide particulate (Al–SiCp) composite. The creep performance of the composite defined by threshold-stress-based creep law by taking the different values of true stress exponent ‘ n ’. It was detected that the trend of stresses and strain rates in the disc was not change on varying the value of the stress exponent but the values of stresses and strain rates in the disc were significantly affected by varying the stress exponent. It was seen that the stresses as well as strain rates in the disc corresponding to $n=5$ lie between the corresponding values estimated using $n=3$ and $n=8$.

You *et al.* [16] described linear variations of Young’s modulus and Poisson’s ratio, and advanced an accurate analytical solution to define deformations and stresses in annular disks made of functionally graded materials subjected to external and internal pressure. Taking mechanical properties of the materials of circular disks to be linear variations, the governing equation was resultant from basic equations of axisymmetric, plane stress problems in elasticity. By changing the governing equation into a hyper geometric equation, an accurate analytical solution of deformations and stresses in circular disks was obtained. The obtained analytical solution was employed to determine the radial displacement and stresses in circular disks subjected to external pressure and internal pressure. It was observed that the radius ratio

was not influence the radial stress. It changed the radial displacement and circumferential stress greatly.

Bayat *et al.* [18] presented a thermo elastic analysis for axis - symmetric rotating disks made of functionally graded material (FGM) with variable thickness. Material properties were supposed to be temperature dependent and graded in the radial direction according to a grading index power law distribution. Semi-analytical solutions for the displacement field were given for solid disk and annular disk under free-free and fixed-free boundary conditions. It was create that a functionally graded rotating disk with concave thickness profile can work more efficiently than the one with uniform thickness irrespective the material properties were assumed to be temperature-dependent or temperature-independent.

Bayat *et al.* [19] attempted to integrate both body and bending forces in the analysis of FG rotating disks. FG rotating disk with inner radius, outer radius, and thickness are axisymmetric with respect to z axis and exposed to mechanical loading. The mechanical loading was attained by pressure load in the z direction and centrifugal load in the radial direction. The material possessions of the constituent components of the disk were assumed to be characterized by a power law distribution along the radial direction in the disk. The first order shear deformation theory was used. A semi-analytical solution for displacement field was given for lesser deflection. Numerical results for normalized displacement and stress resultant components along the radius and thickness of the disk were presented. It was determined that the transverse shear resultants in homogeneous disks were smaller than those in FG disks.

Nie *et al.* [12] defined an infinitesimal deformations of a rotating disk composed of an isotropic linear thermo elastic FGM. Exact solutions for stresses, the hydrostatic pressure and radial displacement for a rotating hollow circular disk with the thickness, the mass density, the thermal expansion coefficient and the shear modulus given by power-law functions of the radius. The analytical solution was given for the case of the shear modulus changing exponentially but constant disk thickness, thermal expansion coefficient. It was originate from numerical results that by fixing the inner surface of a hollow disk reduced the peak hoop stress but increased the maximum radial stress. For a fixed-free hollow disk, the maximum radial stress was greater than the maximum hoop stress. Wrong gradation of the shear modulus, the disk thickness and the mass density can better the maximum radial and hoop stresses as compared to their values for a homogeneous disk of constant thickness.

Bhowmick *et al.* [24] stated numerical solutions under plane stress conditions for elasto-plastic deformation and stress states of rotating solid disks with variable thickness. The problem was expressed by a Variation method. The solution of the governing partial differential equation was attained by assuming a series solution. The formulation was based on von Mises yield criterion and linear strain hardening material performance. The approximate solution was attained by iterative method. It was found that for disk type D1 ($n=2.0$, $k=0.8$) the yield front transmits in a manner to reached root first and then the periphery, whereas for disk type D2 ($n=2.8$, $k=1$) the yield front reached periphery first.

Bayat *et al.* [20] presented a thermo elastic analysis for axis - symmetric rotating disks made of functionally graded material (FGM) with variable thickness. Material properties were expected to be temperature dependent and graded in the radial direction according to a grading index power law distribution. Semi-analytical solutions for the displacement field were assumed for solid disk and annular disk under free-free and fixed-free boundary conditions. It was originate that a functionally graded rotating disk with concave thickness profile can work more efficiently than the one with uniform thickness irrespective of whether the material properties were assumed to be temperature-dependent or temperature-independent.

Deepak *et al.* [9] examined the creep behaviour of functionally graded materials with linearly varying thickness. The creep performance of the composite was given by threshold stress based creep law. The influence of imposing linear particle gradient on the distribution of stresses and strain rates in the composite disc was studied. It was observed that with increase in particle gradient in the disc, the radial stress increases throughout the disc, where the tangential and effective stresses increased near the inner radius but decreased near the outer radius. It was also noticed that the steady state strain rates in the composite disc, have gradient in the distribution of reinforcement, was suggestively lower than that was detected in a disc having uniform distribution of reinforcement.

Sharma *et al.* [25] carried out analysis of a rotating solid disk made of isotropic material with exponentially varying thickness. Transition theory was used to derive the elastic-plastic and transitional stresses. Results achieved were discussed numerically and depicted graphically. It was detected that for disc with exponentially varying thickness ($k=2$), high angular speed was required for initial yielding at internal surface as compared to the flat disc and exponentially varying thickness for $k=4$ onwards. Thus we were decided that flat disc

($C=0.75$) on the safer side of the design requires high percentage increased in angular speed to become fully plastic as compared to the flat disc with the compressible factors ($C=0,0.25,etc.$).

Afsar *et al.* [4] focussed on the finite element analysis of thermo elastic field in a thin circular functionally graded material (FGM) disk was exposed to a thermal load and an inertia force due to rotation of the disk. Due to symmetry, the FGM disk was expected to contained exponential variation of material properties in radial direction only. Based on the two dimensional thermo elastic theories, the axisymmetric problem was expressed in terms of a second order ordinary differential equation which was solved by finite element method. It was originate that the thermo elastic field in an FGM disk was meaningfully influenced by the temperature distribution profile, radial thickness, angular speed, and inner and outer surface temperature difference. It was decided that the thermo elastic field in an FGM disk can be controlled by controlling these parameters.

Deepak *et al.* [10] carried out analysis of steady state creep in rotating disc with different thickness profiles. The disc was to be made of composite consisting of silicon carbide particles embedded in aluminium matrix. The creep performance of the composite was defined by threshold stress based creep law with a stress exponent. The creep stresses and creep rates were expected in different composite discs having linearly varying thickness and hyperbolically varying thickness. The results achieved were matched with those estimated for constant thickness disc to examine the impact of disc profile on creep performance of the composite disc. It was observed that the linearly varying disc was displays the lowest values of stresses and strain rates compared to those detected in hyperbolic or uniform thickness disc.

Zenkour *et al.* [6] presented the exact analytical and numerical solutions for rotating variable-thickness annular disk. The inner and outer edges of the rotating variable-thickness annular disk were considered with boundary conditions. Two different annular disks for the radially varying thickness were given. Both exact and numerical results for stress function, stresses, strains and radial displacement was examined for the first annular disk of variable thickness. Finally, the distributions of stress function, displacement, strains, and stresses were offered. The appropriate comparisons and discussions were completed at the same angular velocity. It was originate that the radial displacement provide minimum value near the inner edge and maximum value near the outer edge for all cases of the parameters k and n . It was also found

that the maximum value of radial stress happened at the inner surface of the disk, while the smallest value at outer surface.

Sharma *et al.* [26] used transition theory to obtain the elastic plastic and transitional stresses. It was observed that the rotating disk made of incompressible material with inclusion required higher angular speed to yield at the internal surface as compared to disk made of compressible material. It was seen that the radial and circumferential stresses were maximum at the internal surface with and without edge load (for flat disk). With the increase in thickness parameter ($k = 2, 4$), the circumferential stress was maximum at the external surface while the radial stress was maximum at the internal surface. It was concluded that the disk made of isotropic compressible material was on the safer side of the design as compared to disk made of isotropic incompressible material as it required higher percentage increase in an angular speed to become fully plastic from its initial yielding.

Das *et al.* [11] presented a large-amplitude free vibration analysis of a rotating annular disk of exponentially varying thickness, exposed to uniform axial pressure. The entire formulation was energy-based and used variational principles to develop the governing equations. The study was supported out up to the onset of yielding, which happened due to the application of two types of external loadings, namely body force due to rotation and uniform axial pressure. The results were matched for three exponential disks having the same mass. The effects of the individual loadings and their combination on the free vibration dynamic performance were presented. It was clear from the study that the dynamic performance of exponential rotating disks of same mass, and of the same inner and outer radii, fluctuates with change in the profile of the disks. The most suitable profile in terms of the dynamic behaviour depends on the design requirements. Therefore, the study provided an insight into the dynamics of the rotating annular disk of variable thickness exposed to uniform axial pressure.

Ali *et al.* [3] presented the elastic solutions of the disk made of functionally graded material (FGM) with variable thickness exposed to rotating load. The material properties were presented by combination of two sigmoid FGM (S-FGM) and disk thickness profile were expected to be signified by power law distributions. Aluminium-ceramic-aluminium FG rotated disk was measured. The results in metal-ceramic-metal FGMs were offered and compared with the known results in the literature. The effects of the material grading index, n , and the geometry of the disk on the stress and displacement were examined. It was originate that a FG disk with concave thickness profile has smaller stresses and displacements

matched with the concave or linear by variable thickness profile. The results proposed that a rotating FG disk with metal-ceramic-metal can be more efficient than the one with ceramic-metal or metal-ceramic. It was also found that for the same grading index, linear thickness profile was the lightest disk followed by convex, concave and constant, respectively.

Hassani *et al.* [14] provided the theoretical and numerical analyses of rotating disks with non-uniform thickness and material properties. Three methods for stress - strain analysis of rotating disks with non-uniform thickness and material properties was exposed to thermo-mechanical loadings was carried out by variable material properties (VMP). The material was expected to be elastic-linear hardening. A power form function was used to define the temperature gradient with the higher temperature at outer surface. It was detected that generally, there exists an excellent agreement between the results. Moreover, it was decided that the RK method provides more correct results than the VMP method for coarser mesh, but the VMP method was seen to be easier to implement, required less CPU time and computer hardware.

Thakur *et al.* [22] applied Seth's transition theory to the problems of thickness variation parameter in a thin rotating disc by finite deformation. The results found were relevant to compressible materials. It was seen that the flat disc of compressible materials required higher percentage improved in angular speed to become fully plastic as matched to disc made of incompressible material. The effect of thickness on circumferential stresses was maximum at the external surface for compressible materials as compared to incompressible materials whereas for flats disc circumferential stresses were maximum at the internal surface for incompressible material as compared to compressible materials.

PROBLEM FORMULATION

After going through the literature some gaps were observed in the research area.

3.1 Gaps in the Literature:

It was observed that the work was done on the rotating disc for constant thickness. There has been little work on the rotating disc of variable thickness which is stated in the literature.

3.2 Purposed Work

Rotating discs[27] have been getting significant attention due its wide range of engineering applications in rotating machinery including turbines, pumps, compressors, flywheels, braking system of automobiles, railway and aerospace, computer disc drives etc. In most of these applications, the disc is exposed to severe mechanical and thermal loadings as it has to function at elevated temperatures. This makes the disc material undergo creep deformations. The excellent mechanical properties like high specific strength/stiffness and high temperature stability presented by aluminium/aluminium alloy based composites consisting of silicon carbide particles/whiskers or fibers make them appropriate material for use in rotating disc applications.

The evaluation tells that studies relating to creep behaviour of rotating composite disc of constant thickness are presented in literature. However, the studies related to creep performance of a composite disc having variable thickness are rather scant. It is seen that by changing the disc profile the stresses in the disc may be reduced significantly. Therefore, it is decided to carry out a study pertaining to steady state creep behaviour of a rotating composite disc having variable thickness. The objective of the study will be to investigate the effect of varying the disc profile for the same volume of the disc on the steady state creep behaviour of the composite disc.

3.3 Methodology

The work was carried out as per the following steps:

- i) First of all, constitutive equations for multi-axial creep were developed.
- ii) After that equilibrium equation along with these equations were solved.
- iii) Then a code was written in 'c' language, to determine various results.
- iv) After obtaining the results, analysis has been carried out to draw important conclusion.

MATHEMATICAL ANALYSIS OF CREEP

In this chapter a mathematical model is developed to describe steady state creep behaviour of a rotating composite disc having variable thickness. The creep performance of the disc material has been defined by threshold stress based creep law. The model developed has been used to determine the stress and strain rate distributions for composite having different types of disc profiles.

4.1 Assumptions

A composite disc made of Al-SiC_p with inner and outer radii of 'a' and 'b' respectively, having thickness 'h' and rotating at an angular velocity of 'x' (radian/sec). For the purpose of investigation the following assumptions are made:

- (i) The disc material is incompressible, isotropic and possesses uniform distribution of SiC_p in aluminium matrix.
- (ii) Stresses at any point in the disc remain constant with time i. e. steady state condition of stress is expected.
- (iii) Elastic deformations in the disc are small and neglected as compared to creep deformations.
- (iv) The thickness of disc is very small compared to its diameter, therefore the axial stress (σ_z) throughout the disc may be assumed zero.
- (v) The material of the rotating disc is expected to undergo steady state creep according to the well documented creep law given by:

$$\dot{\bar{\epsilon}} = [M(\bar{\sigma} - \sigma_0)]^n \quad (4.1)$$

$$\text{Where } M = \frac{1}{E} (A' \exp \frac{-Q}{RT})^{1/n}$$

where the symbols $\bar{\epsilon}$, $\bar{\sigma}$, σ_0 , A' , n , Q , E , R , and T denote respectively the effective strain rate, effective stress, threshold stress, structure dependent parameter, true stress exponent, true

activation energy, temperature-dependent, Young's modulus, gas constant and operating temperature.

(vi) Material of the disc yield according to the Tresca Yield Criterion.

4.2 Maximum Shear Stress Criterion (Tresca Yield Criterion)

The criterion assumes that yielding occurs when the maximum shear stress reaches the value of the shear stress in the uniaxial tension test. The maximum shear stress [30] is given by,

$$\tau_{\max} = \frac{\sigma_1 - \sigma_3}{2}$$

Where, σ_1 is the algebraically largest and σ_3 is the algebraically smallest principal stress. For uniaxial tension, $\sigma_1 = \sigma_y$, $\sigma_2 = \sigma_3 = 0$ and the shearing yield stress τ_y is equal to $\sigma_y/2$.

Therefore, the above equation becomes, $\frac{\sigma_1 - \sigma_3}{2}$

$$\tau_{\max} = \frac{\sigma_1 - \sigma_3}{2} = \tau_y = \frac{\sigma_y}{2}$$

Therefore, the maximum shear stress criterion is given by

$$\sigma_1 - \sigma_3 = \sigma_y$$

For a state of pure shear, $\sigma_1 = -\sigma_3 = k$, $\sigma_2 = 0$, the maximum shear stress criterion predicts that yielding will occur when,

$$\sigma_1 - \sigma_3 = 2k = \sigma_y$$

This equation can be rewritten as,

$$K = \frac{\sigma_y}{2}$$

Hence, the maximum shear stress criterion may be written as,

$$\sigma_1 - \sigma_3 = 2k$$

4.3 Analysis of Creep

Consider a thin isotropic composite disc of 6061Al-SiC_w of density ρ and rotating at a constant angular speed ' ω '. The disc thickness is expected to be ' h ' and ' a ' and ' b ' be the inner and outer radii of the disc, respectively.

Let A and A_0 denote the areas of transverse section of the disc element with outer radii ' r ' and ' b ' respectively but having the same inner radius ' a '. The A and A_0 may be written as, [10]

$$A = \int_a^r h \, dr \quad (4.2)$$

$$A_0 = \int_a^b h \, dr \quad (4.3)$$

The polar moment of area I and I_0 of these disc elements having outer radii ' r ' and ' b ' respectively but with inner radius ' a ' may be stated as, [10]

$$I = \int_a^r hr^2 \, dr \quad (4.4)$$

$$I_0 = \int_a^b hr^2 \, dr \quad (4.5)$$

The average tangential stress in the disc, $\sigma_{\theta av}$ may be defined as, [10]

$$\sigma_{\theta av} = 1/A_0 \int_a^b h \sigma_{\theta} \, dr \quad (4.6)$$

The generalized constitutive equations for creep in an isotropic composite under biaxial state of stress (i.e. $\sigma_z=0$) takes the following form when reference frame is along the principal directions r , θ and z .

$$\dot{\epsilon}_r = \frac{\dot{\epsilon}}{2\bar{\sigma}} (2\sigma_r - \sigma_{\theta}) \quad (4.7)$$

$$\dot{\epsilon}_{\theta} = \frac{\dot{\epsilon}}{2\bar{\sigma}} (2\sigma_{\theta} - \sigma_r) \quad (4.8)$$

$$\dot{\epsilon}_z = \frac{\dot{\epsilon}}{2\bar{\sigma}} (-\sigma_r - \sigma_{\theta}) \quad (4.9)$$

where $\dot{\epsilon}_r, \dot{\epsilon}_\theta, \dot{\epsilon}_z$ and $\sigma_r, \sigma_\theta, \sigma_z$ are the respective strain rates and the stresses in the directions r, θ and z, as indicated by the subscripts.

According to Tresca yield criterion the effective stress:

$$\bar{\sigma} = \sigma_\theta$$

Putting the values of $\dot{\bar{\epsilon}}$ from equation (4.1) and σ_θ in equation (4.7)

$$\dot{\epsilon}_r = \frac{d\dot{u}_r}{dr} = \frac{[M(\bar{\sigma} - \sigma_0)]^n}{2\sigma_\theta} (2\sigma_r - \sigma_\theta)$$

Multiplying and dividing by σ_θ

$$\frac{d\dot{u}_r}{dr} = \frac{[M(\bar{\sigma} - \sigma_0)]^n}{2\sigma_\theta} \left(2 \left(\frac{\sigma_r}{\sigma_\theta} \right) - \left(\frac{\sigma_\theta}{\sigma_\theta} \right) \right) \sigma_\theta$$

Put $\frac{\sigma_r}{\sigma_\theta} = x$

$$\frac{d\dot{u}_r}{dr} = \frac{(2x-1)}{2} [M(\bar{\sigma} - \sigma_0)]^n \quad (4.10)$$

Similar lily putting the values of $\dot{\bar{\epsilon}}$ and σ_θ in equation (4.8)

$$\dot{\epsilon}_\theta = \frac{\dot{u}_r}{r} = \frac{[M(\bar{\sigma} - \sigma_0)]^n}{2\sigma_\theta} (2\sigma_\theta - \sigma_r)$$

and

$$\dot{\epsilon}_z = -(\dot{\epsilon}_\theta + \dot{\epsilon}_r)$$

$$\frac{\dot{u}_r}{r} = \dot{\epsilon}_\theta = \frac{(2-x)}{2} [M(\bar{\sigma} - \sigma_0)]^n \quad (4.11)$$

From Eq. (4.10) and Eq. (4.11),

$$\frac{d\dot{u}_r}{dr} \frac{r}{\dot{u}_r} = \frac{(2x-1)}{(2-x)}$$

$$\frac{d\dot{u}_r}{\dot{u}_r} = \frac{\phi(r)}{r} dr \quad (4.12)$$

Where $\phi(r) = \frac{(2x-1)}{(2-x)}$

Integrating Eq. (4,12) from limits 'a' to 'r',

$$\int_a^r \frac{d\dot{u}_r}{\dot{u}_r} = \int_a^r \frac{\phi(r)}{r} dr$$

$$|\log \dot{u}_r|_a^r = \int_a^r \frac{\phi(r)}{r} dr$$

$$(\log \dot{u}_r - \log \dot{u}_a) = \int_a^r \frac{\phi(r)}{r} dr$$

$$\log \frac{\dot{u}_r}{\dot{u}_a} = \int_a^r \frac{\phi(r)}{r} dr$$

Now taking antilog on both sides

$$\frac{\dot{u}_r}{\dot{u}_a} = \exp \left[\int_a^r \frac{\phi(r)}{r} dr \right]$$

$$\dot{u}_r = \dot{u}_a \exp \left[\int_a^r \frac{\phi(r)}{r} dr \right] \quad (4.13)$$

Substituting the value of \dot{u}_r in Eq. (4.11)

$$\frac{\dot{u}_a}{r} \cdot \exp \left[\int_a^r \frac{\phi(r)}{r} \cdot dr \right] = \frac{(2-x)}{2} [M(\bar{\sigma} - \sigma_0)]^n$$

$$\frac{\dot{u}_a}{r} \cdot \frac{2}{(2-x)} \cdot \exp \left[\int_a^r \frac{\phi(r)}{r} dr \right] = [M(\bar{\sigma} - \sigma_0)]^n$$

$$u_a^{1/n} \psi(r)^{1/n} = [M(\bar{\sigma} - \sigma_0)]^n$$

$$\text{Where } \psi(r)^{1/n} = \frac{1}{r^{(2-x)}} \cdot \exp \left[\int_a^r \frac{\phi(r)}{r} dr \right] \quad (4.14)$$

$$\frac{[u_a \psi(r)^{1/n}]^{\frac{1}{n}}}{M} = (\bar{\sigma} - \sigma_0)$$

$$\frac{u_a^{1/n} \psi(r)^{1/n}}{M} = (\bar{\sigma} - \sigma_0)$$

$$\bar{\sigma} = \frac{u_a^{1/n} \psi(r)^{1/n}}{M} + \sigma_0$$

But according to Tresca yield theory, $\bar{\sigma} = \sigma_\theta$

$$\text{So the above expression becomes } \sigma_\theta = \frac{u_a^{1/n} \psi(r)^{1/n}}{M} + \sigma_0 \quad (4.15)$$

4.4 Equilibrium Equation for Rotating Disc

Let us consider an element of the disc, as shown in Fig. 4.2, between radius r and $(r+dr)$ and subtending an angle $d\theta$ at the centre of the disc 'O'. Say the thickness of the disc at radial distance r and $(r+dr)$ be h and $(h+dh)$ respectively.

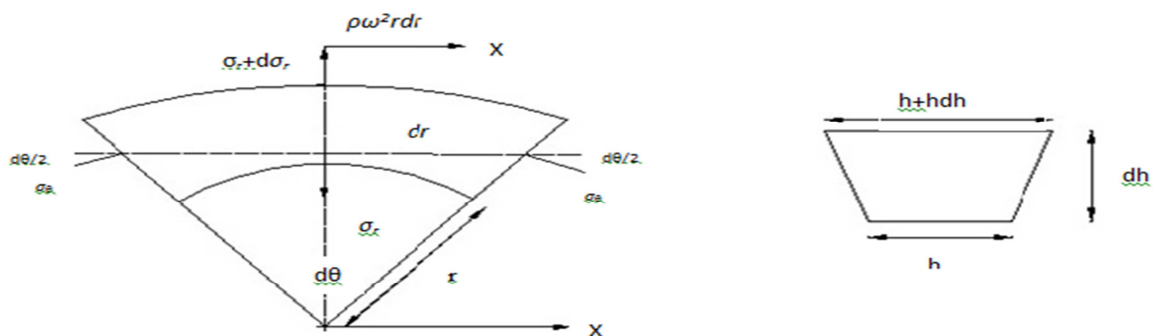


Fig 4.1: Free body diagram of an element of the disc.

Resolving the forces acting on the disc element along the vertical direction, i.e. $\Sigma v = 0$ implies,

$$\left[\sigma_r + \frac{d\sigma_r}{dr} \cdot dr\right] \cdot [r+dr] \cdot [d\theta] \cdot [h+dh] - \sigma_r \cdot r \cdot d\theta \cdot h - \left[2 \cdot \sigma_\theta \cdot \frac{d\theta}{2}\right] \cdot [2h+dh] \cdot \frac{dr}{2} + \rho \cdot r \cdot \omega^2 [2h+dh] \cdot \left[r + \frac{dr}{2}\right] \cdot \left[\frac{d\theta}{2}\right] \cdot d\theta = 0$$

Neglecting the smaller term from above equation and simplifying, we get

$$\frac{d}{dr} [\sigma_r \cdot r \cdot h] - \sigma_\theta \cdot h - \rho \cdot r^2 \cdot \omega^2 \cdot h = 0 \quad (4.16)$$

The above equation is the equation of equilibrium for the rotating disc of variable thickness.

Where, $\rho = \text{density of the composite}$

$\omega^2 = \text{Angular velocity}$

$r = \text{radius of the disc such that } (a < r < b)$

Multiplying the above equation (4.16) by dr

$$d(r \cdot \sigma_r \cdot h) - \sigma_\theta \cdot h \cdot dr + \rho \omega^2 r^2 \cdot h \cdot dr = 0$$

Integrating it from limits a to b ,

$$\int_a^b d(r \cdot \sigma_r \cdot h) - \int_a^b \sigma_\theta \cdot h \cdot dr + \int_a^b \rho \omega^2 r^2 \cdot h \cdot dr = 0$$

$$[h \cdot r \cdot \sigma_r]_a^b - \int_a^b \sigma_\theta \cdot h \cdot dr + \rho \omega^2 \cdot I_0 = 0$$

Where $I_0 = \int_a^b r^2 \cdot h \cdot dr$

$$[h_b \cdot r_b \cdot \sigma_{rb} - h_a \cdot r_a \cdot \sigma_{ra}] - \int_a^b \sigma_\theta \cdot h \cdot dr + \rho \omega^2 \cdot I_0 = 0 \quad (4.17)$$

Dividing Eqn. (4.17) by A_0 , and rearranging the terms we can get the average tangential stress, defined in Eqn. (4.6), as,

$$\sigma_{\theta \text{avg}} = \frac{1}{A_0} \int_a^b \sigma_\theta \cdot h \cdot dr = \frac{(h_b \cdot r_b \cdot \sigma_{rb})}{A_0} - \frac{(h_a \cdot r_a \cdot \sigma_{ra})}{A_0} + \frac{\rho \cdot \omega^2 \cdot I_0}{A_0}$$

$$\sigma_{\theta\text{avg}} = \frac{1}{A_0} \int_a^b \sigma_{\theta} \cdot h \cdot dr = \frac{(h_b \cdot r_b \cdot \sigma_{rb} - h_a \cdot r_a \cdot \sigma_{ra} + \rho \cdot \omega^2 \cdot I_0)}{A_0}$$

$$\sigma_{\theta\text{avg}} = \frac{1}{A_0} \int_a^b \sigma_{\theta} \cdot h \cdot dr \quad (4.18)$$

$$\sigma_{\theta\text{avg}} = \frac{(h_b \cdot r_b \cdot \sigma_{rb} - h_a \cdot r_a \cdot \sigma_{ra} + \rho \cdot \omega^2 \cdot I_0)}{A_0} \quad (4.19)$$

where, h_a and h_b denote the thickness of the disc respectively at the inner and the outer radii, and σ_{ra} and σ_{rb} are the radial stresses at the inner and outer radii respectively. substitute σ_{θ} from equation (4.15) into equation (4.18)

$$\sigma_{\theta\text{avg}} = \frac{1}{A_0} \int_a^b \left[\frac{u_a^{1/n} \psi(r)^{1/n}}{M} + \sigma_0 \right] \cdot h \cdot dr$$

The above equation can be simplified as,

$$\frac{u_a^{1/n}}{M} = \frac{A_0 \cdot \sigma_{\theta\text{avg}} - \int_a^b \sigma_0 \cdot h \cdot dr}{\int_a^b \psi(r)^{1/n} \cdot h \cdot dr}$$

Put the value of $\sigma_{\theta\text{avg}}$ from equation (4.19) into $\frac{u_a^{1/n}}{M}$

$$\frac{u_a^{1/n}}{M} = \frac{(h_b \cdot r_b \cdot \sigma_{rb} - h_a \cdot r_a \cdot \sigma_{ra} + \rho \cdot \omega^2 \cdot I_0) - \int_a^b \sigma_0 \cdot h \cdot dr}{\int_a^b \psi(r)^{1/n} \cdot h \cdot dr} \quad (4.20)$$

It is important to mention that the radial stresses σ_{ra} and σ_{rb} at the inner and the outer radii, respectively are zero due the imposed boundary conditions:

$$\sigma_r = 0 \text{ at } r = a$$

$$\sigma_r = 0 \text{ at } r = b$$

Put the value of $\frac{u_a^{1/n}}{M}$ in equation (4.15) we get,

$$\sigma_{\theta} = \frac{A_0 \cdot \sigma_{\theta\text{avg}} - \int_a^b \sigma_0 \cdot h \cdot dr}{\int_a^b \psi(r)^{1/n} \cdot h \cdot dr} + \sigma_0 \quad (4.21)$$

In the first iteration, it is assumed that $\sigma_{\theta\text{av}} = \sigma_{\theta}$ over the entire disc radii. The $\sigma_{\theta\text{av}}$

can be obtained from Eqn. (4.19) given above.

Now again multiplying the equilibrium equation of rotating disc by dr both sides,

$$d(r \cdot \sigma_r \cdot h) - \sigma_\theta dr \cdot h + \rho \omega^2 r^2 \cdot h \cdot dr = 0$$

Integrating it from limits a to r ,

$$\int_a^r d(r \cdot \sigma_r \cdot h) - \int_a^r \sigma_\theta \cdot h dr + \int_a^r \rho \omega^2 r^2 \cdot h dr = 0$$

$$[r \cdot \sigma_r \cdot h]_a^r = \int_a^r \sigma_\theta \cdot h dr + \rho \omega^2 \int_a^r r^2 \cdot h dr$$

$$[r \cdot \sigma_r \cdot h - a \cdot \sigma_a \cdot h] = \int_a^r \sigma_\theta \cdot h dr + \rho \omega^2 \int_a^r r^2 \cdot h dr$$

By applying the boundary conditions to the above equation,

$$[r \cdot \sigma_r \cdot h - 0] = \int_a^r \sigma_\theta \cdot h dr + \rho \omega^2 \int_a^r r^2 \cdot h dr$$

$$\sigma_r = \frac{1}{r \cdot h} \left[\int_a^r \sigma_\theta \cdot h dr + \rho \omega^2 \int_a^r r^2 \cdot h dr \right]$$

$$\sigma_r = \frac{1}{r \cdot h} \left[\int_a^r \sigma_\theta \cdot h dr + \rho \omega^2 I \right] \quad (4.22)$$

Where the term I has been already defined in Eqn. (4.5).

$$I = \int_a^r h r^2 dr$$

Knowing σ_θ and σ_r , the stress ratio, $x = \sigma_r / \sigma_\theta$ can be calculated and hence second approximation for σ_θ , may be calculated from Eqn. (4.15) which can be again used to in Eqn. (4.22) to obtain the second approximation of σ_r . The process is carried out till the convergence is achieved. Once the distributions of radial and tangential stress are known, the strain rates in the disc may be calculated from Eqs. (4.7) and (4.8).

4.5 Disc Profile

The creep response of rotating disc is determined by variation in thickness profile of the disc. For this study profile of disc which can be used for linear and non-linear varying thickness by setting the different value of geometric parameters for different profiles of the disc used in the equation. The profile function [17] considers here is given by the equation:

$$h(r)=h_a[1-n\left(\frac{r}{b}\right)^k] \quad (4.23)$$

where 'n' and 'k' are the geometric parameters ($0 \leq n < 1, k > 0$), h_a is the thickness at the axis of disc, and 'b' is the radius of disc. The variability of the thickness is in the radial direction thickness of the disc is very small compared to its diameter. With the help of this type of profile function we can create different types of disc profiles: [17]

- (i) Disc with uniform thickness: For uniform thickness $n=0$.
- (ii) Disc with linear varying thickness: For this type of linear decreasing thickness is obtained by setting $k=1$ and $n \neq 0$ in the above equation:

$$h(r)=h_a[1-n\left(\frac{r}{b}\right)]$$

The thickness of the disc at the axis is given by $h_a=43.217\text{mm}$ and thickness of the disc at the outer radius $h_b=13.97\text{mm}$. The value of geometric parameter taken as $n=0.4$.

- (iii) Disc with non-linear varying thickness: For non-linear variable thickness, we obtained two types of thickness profiles:
 - a) Concave
 - b) Convex

For concave profile geometric parameter is given by $k < 1$ and for convex profile $k > 1$.

For concave we take the value of $k=0.55$ and value of $n=0.4$.

For convex we take the value of $k=2$ and value of $n=0.4$.

Taking the thickness of the disc at the inner radius, h_a , and at the outer radius, h_b , as 43.217 mm and 13.97 mm respectively, it is important to mention here that the thickness of both the discs at the inner and the outer radii are selected in such a manner that both the disc has same volume. The inner and the outer radii of all the discs are taken as 31.75 mm and 152.4 mm respectively.

4.6 Calculation of Area and Inertia of Discs

Using Eq. (4.23) in Eqns. (4.2), (4.3), (4.4), (4.5) the values of A, A₀, I and I₀ may be calculated. The values obtained are given as below,

$$A_0 = h_a * [(b-a) - n * (b^{k+1} - a^{k+1}) / ((k+1) * b^k)]$$

$$I_0 = h_a * [(b^3 - a^3) / 3 - n * (b^{k+3} - a^{k+3}) / ((b)^k * (k+3))]$$

$$A = h_a * [(r-a) - n * (r^{k+1} - a^{k+1}) / ((k+1) * (b)^k)]$$

$$I = h_a * [(r^3 - a^3) / 3 - n * (r^{k+3} - a^{k+3}) / ((b)^k * (k+3))]$$

The values of A, A₀, I and I₀ obtained above for the discs having different profile may be used in the analysis described in section 4.4 to calculate the stress and strain rate distributions in the different discs.

4.7 Solution Procedure

The stress distribution is evaluated from the above analysis by iterative numerical scheme of computation. To begin with, we calculate the average tangential stress in the disc, given by

$$\sigma_{\theta av} = 1/A_0 \int_a^b h \sigma_{\theta} dr$$

To find the first approximation of x, to be used in Eq. (4.14), we assume that $\sigma_{\theta} = \sigma_{\theta av}$ in Eq. (4.22) to obtain the first approximation of σ_r i.e. $[\sigma_r]_1$. Dividing $[\sigma_r]_1$ by $\sigma_{\theta av}$, we get $[x]_1$, which is substituted in Eq. (4.14) for x to get $[\psi]_1$ using $[\psi]_1$ in eq. (4.21) $[\sigma_{\theta}]_1$ is obtained.

On substituting $[\sigma_{\theta}]_1$, for $[\sigma_{\theta}]$, in Eq. (4.22), the second approximation of σ_r i. e. $[\sigma_r]_2$ is found, which is used to find the second approximation of x, i. e., $[x]_2$. The iteration is continued till the process converges yielding the values of stresses at different points of the radius grid. For rapid convergence 75% of the value of σ_{θ} obtained in the current iteration have been mixed with 25% of the value of σ_{θ} obtained in the previous iteration and this modified value is used in the next iteration. Thereafter, the radial and tangential strain rates in the disc are calculated respectively from Eqs. (4.10) and (4.11).

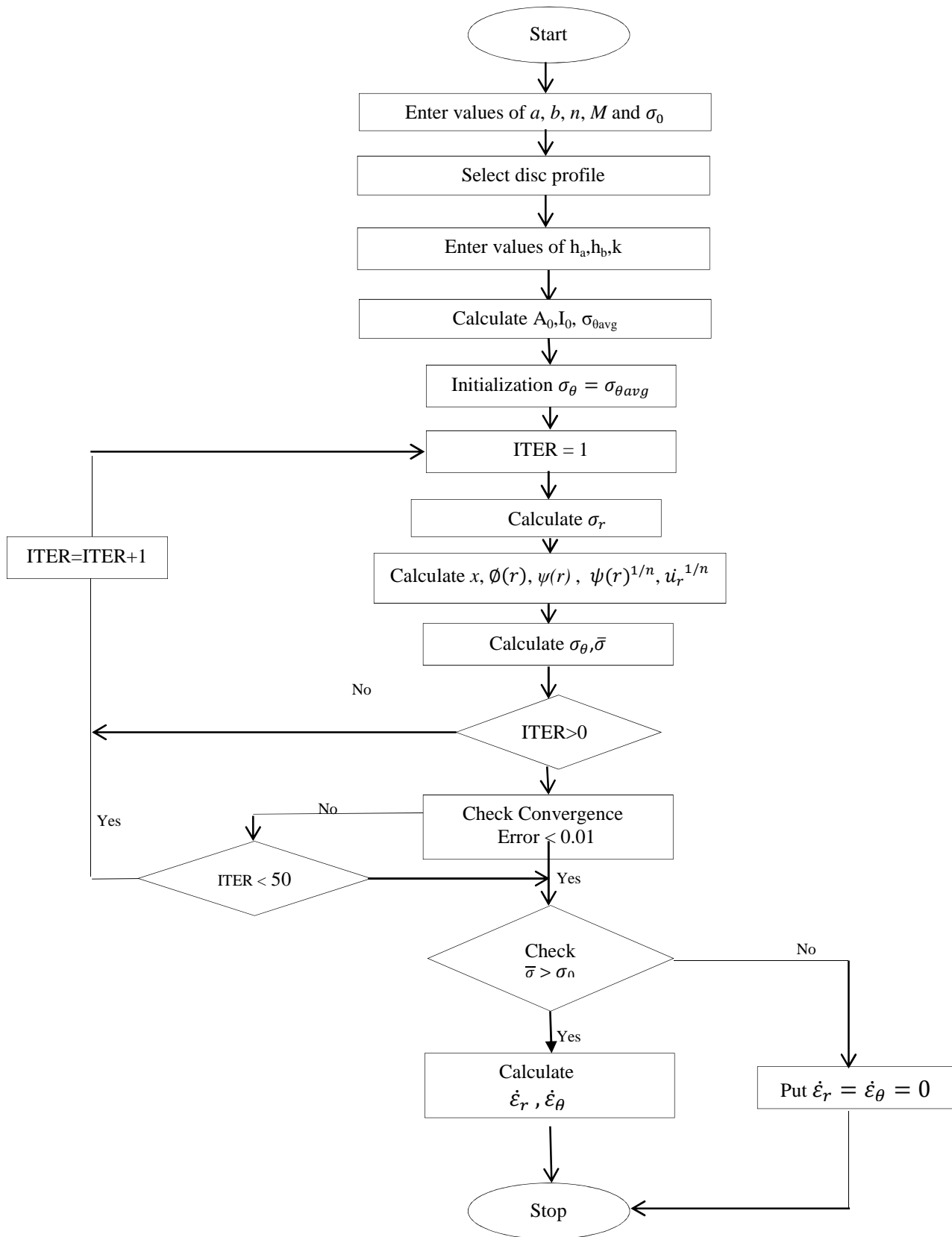


Fig 4.2: Numerical scheme of computation.

RESULTS AND DISCUSSIONS

Numerical calculations, based on the analysis presented in the previous chapter have been carried out to obtain steady state creep response of the composite disc for different thickness profiles. A computer program based on the mathematical formulation has been developed to achieve the distribution of stresses and steady state creep rates in the rotating discs with different profiles. The different thickness profiles are achieved from the profile function give. The thicknesses profiles obtained from the equation are for constant thickness, linear variable, concave thickness profile and for convex thickness profile. The material of the disc is Al-SiC_p which undergoes steady state creep. The effect of disc profile has been examined on the creep behaviour of the isotropic (Al-SiC_p). The effects of using different disc profiles on the creep behaviour of the discs are discussed separately.

5.1 VALIDATION

Before discussing the result it is necessary to check the results and the software developed. For this purpose radial stress are calculated for a rotating composite disc. The operating conditions, dimensions and creep parameters of the composite disc are stated in Table: 5.1.

Table: 5.1 Parameters and operating conditions for composite disc.

Parameters for Composite Disc	
Density of the Material (ρ)	$\rho = 2750.01 \text{ kg m}^{-3}$
Disc radius: Inner(a) and Outer Radius(b)	$a = 31.75 \text{ mm}, b = 152.4 \text{ mm}$
Thickness at Inner(h_a) and Outer Radius(h_b)	$h_a = 43.217, h_b = 13.97$
Creep Parameter, M	$M = 0.00432 \text{ s}^{-1/5} / \text{MPa}$
Stress Exponent, n	$n = 5$
Threshold Stress (σ_0)	$\sigma_0 = 19.46 \text{ MPa}$
Particle Size (P)	$P = 1.7 \text{ }\mu\text{m}$
Volume Content (V)	$V = 10 \%$
Operating Conditions	
Disc rpm	15000
Operating Temperature, T	623.00 K

These parameters are used in computer code to calculate the stress, strains in composite disc. The results achieved are compared with the published results [10]. Fig 5.1 shows the good agreement between the results obtained by the procedure outlined in this study and the published results [10] for a rotating composite disc.

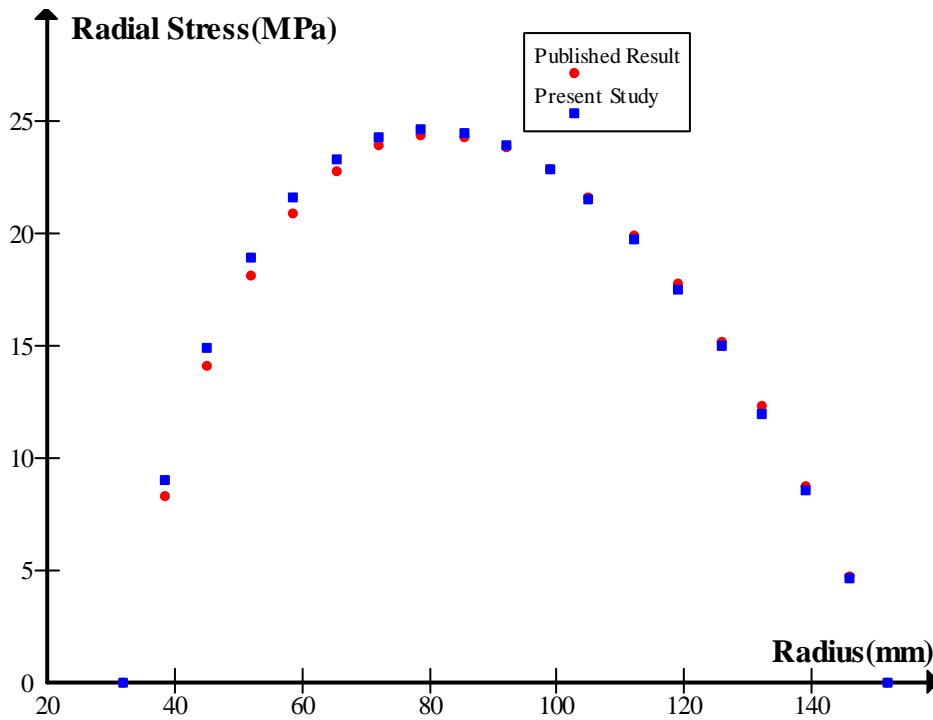


Fig 5.1: Comparison of present study and the published results for radial stress.

5.2 Effect of Disc Profile on Creep Behaviour of Disc

Figs. 5.2-5.6 show the effect of varying the disc thickness on the creep performance of the composite disc made of isotropic material (6061Al- 20% vol SiC_p). The disc is estimated to operate at 623 K.

We compare four types thickness profile. These are uniform thickness disc, linear varying thickness, concave and convex thickness profiles. For uniform thickness profile the value of $n=0$ for eqn.(4.23).where 'n' and 'k' are the geometric parameters. It is to be noted that the parameter n determines the thickness at the outer edge of the annular disk relative to h_0 while the parameter k determine the shape of the profile. The value of k equal to unity represents a linearly variable thickness for the disk. For concave profile disc the value of is $k<1$ and for convex the value of is $k>1$.

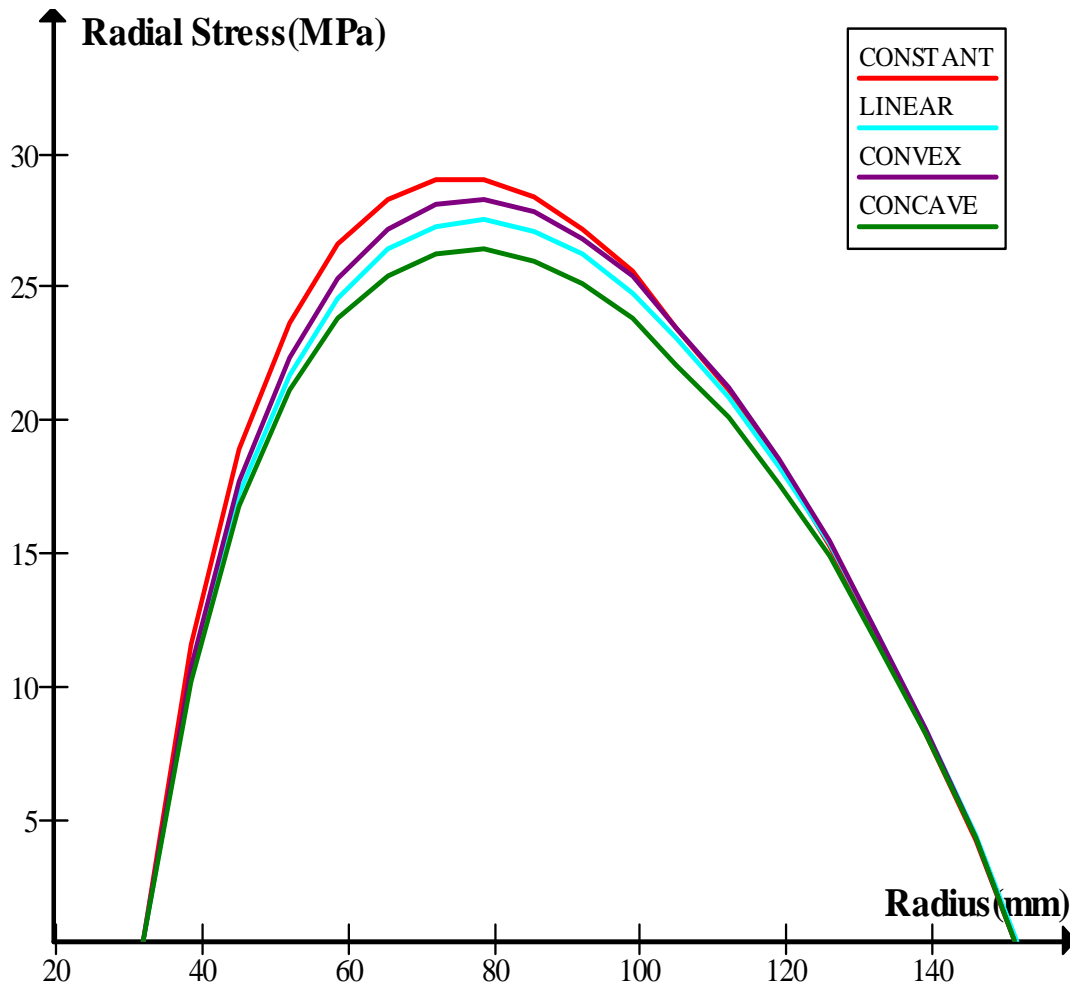


Fig 5.2: Effects of disc thickness on radial stress.

The radial stress as shown in Fig. 5.2, increases from zero at the inner radius, touches maximum before dropping to zero again at the outer radius under the imposed boundary conditions of radial stress vanishing at both the inner radius and the outer radius. The radial stress in the disc with linearly varying thickness is reduced everywhere compared to disc of uniform thickness. Concave thickness profile has smaller stresses in comparison to disks with linear or convex thickness profiles.

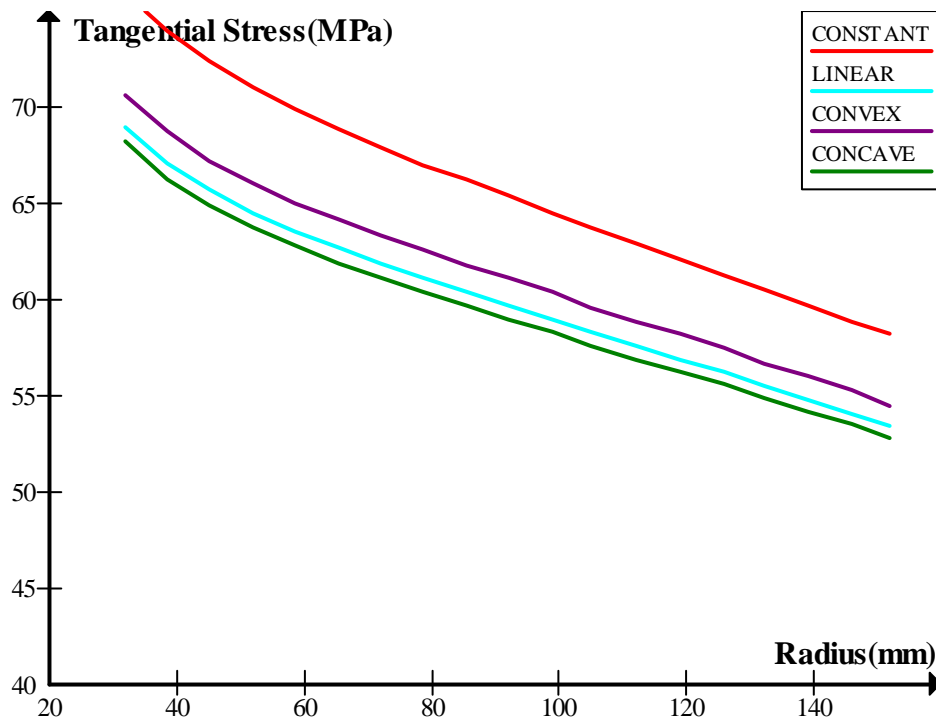


Fig 5.3: Effects of disc thickness on tangential stress.

The tangential stress as shown in Fig 5.3 decreases on as move from the inner radius to the outer radius of the disc. The tangential stress in the disc having linearly varying thickness decreases over the entire disc radii when compared to composite disc having uniform thickness. The disc having concave and convex varying thickness displays the lowest values of tangential stress over the entire radius compared to uniform thickness disc. Therefore, it is obvious that by increasing and decreasing the disc thickness respectively near the inner and the outer radii, compared to uniform thickness, the tangential stress in the disc could be reduced to a significant extent.

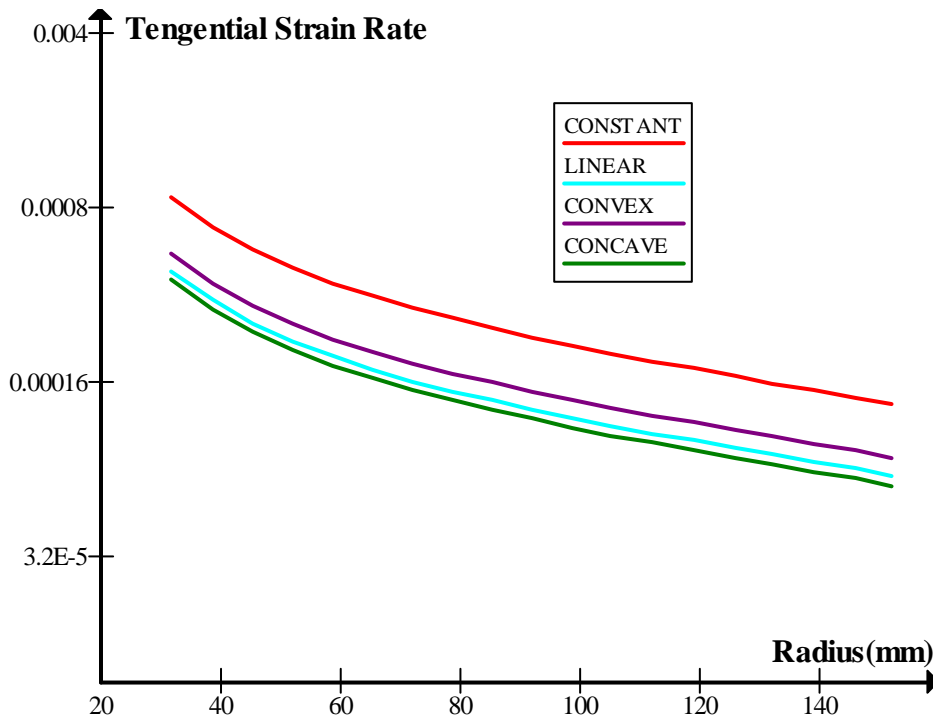


Fig 5.4: Effects of disc thickness on tangential strain rate.

Fig 5.4 shows the effect of disc profile on tangential strain rate. The tangential strain rate is maximum at inner radius and goes on decreasing as moves towards the outer radius. The tangential strain rates in the linearly varying disc, concave and convex profile varying discs are reduced in magnitude compared to those observed in uniform thickness disc. The distribution of strain rate is relatively more uniform in disc having variable thickness, which may be lead to the reduction in distortion of the disc.

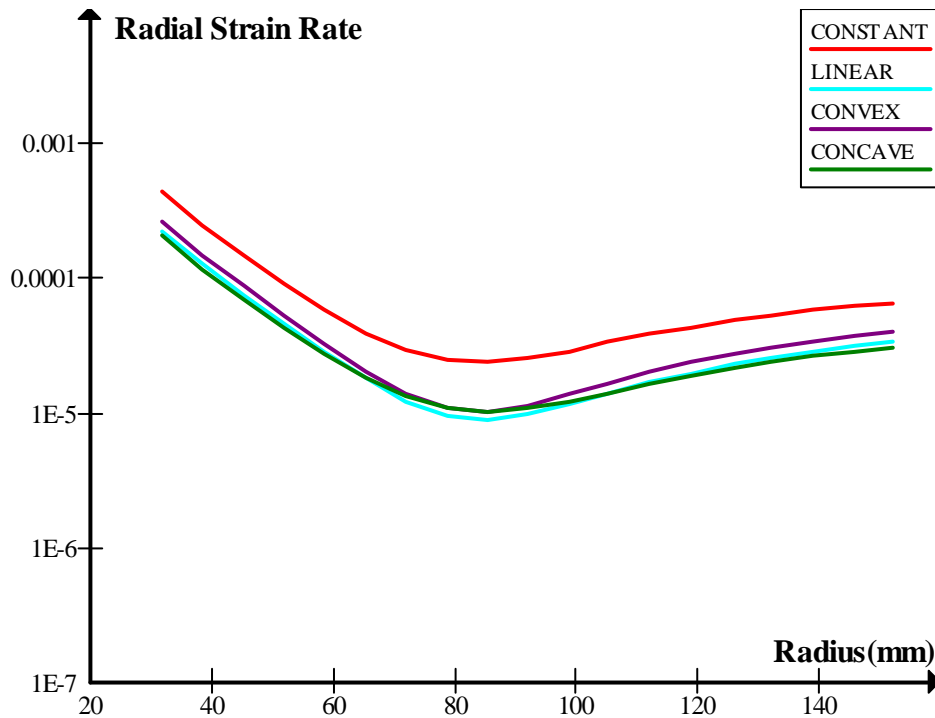


Fig 5.5: Effects of disc thickness on radial strain rate.

The radial strain rate shown in Fig 5.5 is meaningfully affected by varying the disc profile. The radial strain rates is maximum at inner radius and goes on decreasing with radial distance up to certain distance, followed by a slight increase towards the outer radius. As estimated, over the entire radius the radial strain rate corresponding to uniform thickness disc is the highest and is lower for linearly varying thickness, concave and convex profile disc. It is minimum near the middle region of the disc for linear varying thickness disc.

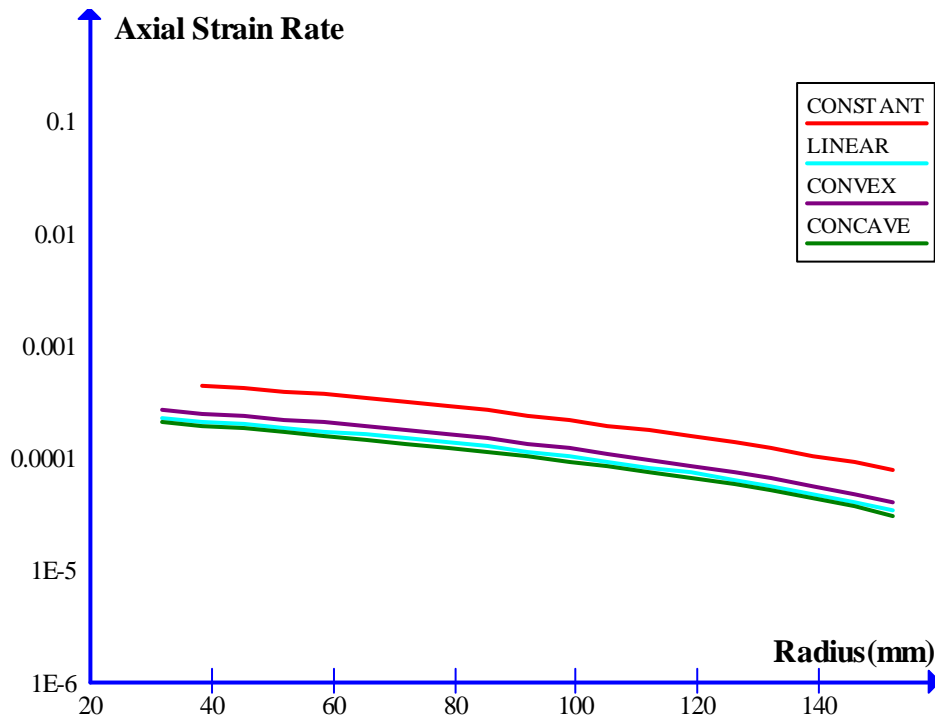


Fig 5.6: Effects of disc thickness on axial strain rate.

Fig 5.6 shows the axial strain rate performance for different disc profiles. It is clear that the axial strain rate is decreasing continuously from inner to outer radius of the disc. For constant profile axial strain rate is higher than linear, concave and convex profiles. Concave profile has less axial strain rate than the other profiles.

From above conversation it appears that the strain rates in the disc can be significantly reduced by using disc with variable thickness having more thickness at the inner radius and lesser thickness at the outer radius as compared to disc having uniform thickness.

5.3 Effect of Varying Particle Size on Creep Behaviour of Composite Disc

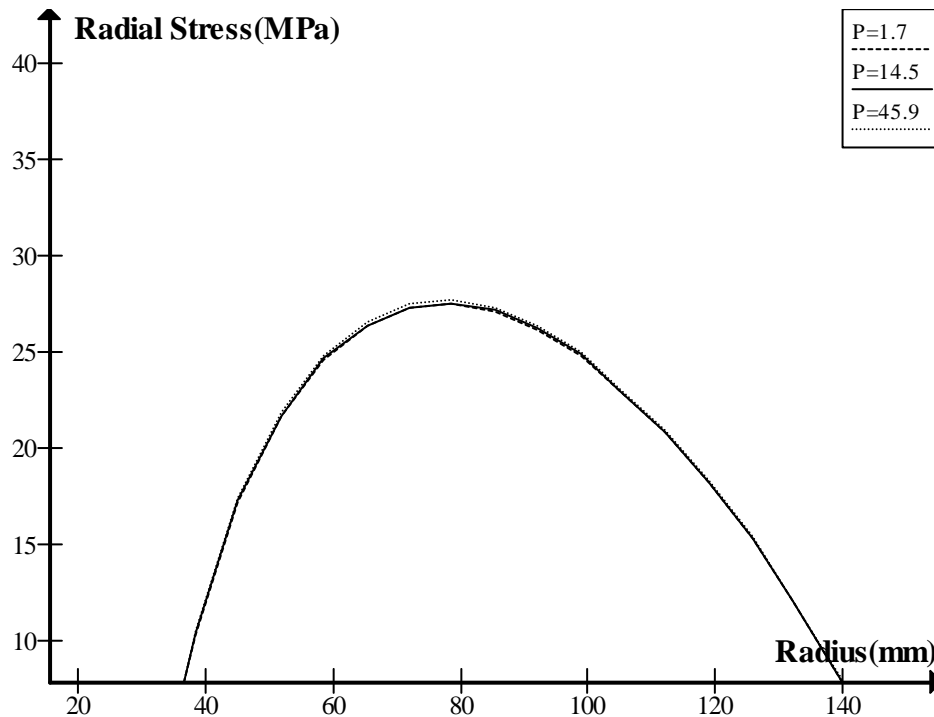


Fig 5.7: Effects of varying particle size of dispersoids (SiC_p) on radial stress.

Fig 5.7 shows the effect of particle size on the radial stress for linear varying thickness disc profile. Here we take three types of the size of the particles [27] i.e. 1.7 μm , 14.5 μm and 45.9 μm . Radial stresses are increasing from inner to outer radius and high at the middle of the disc and remain zero at inner and outer radius due to imposed boundary conditions. From the above results, it seems that the effect of particle size on the radial stress is very small.

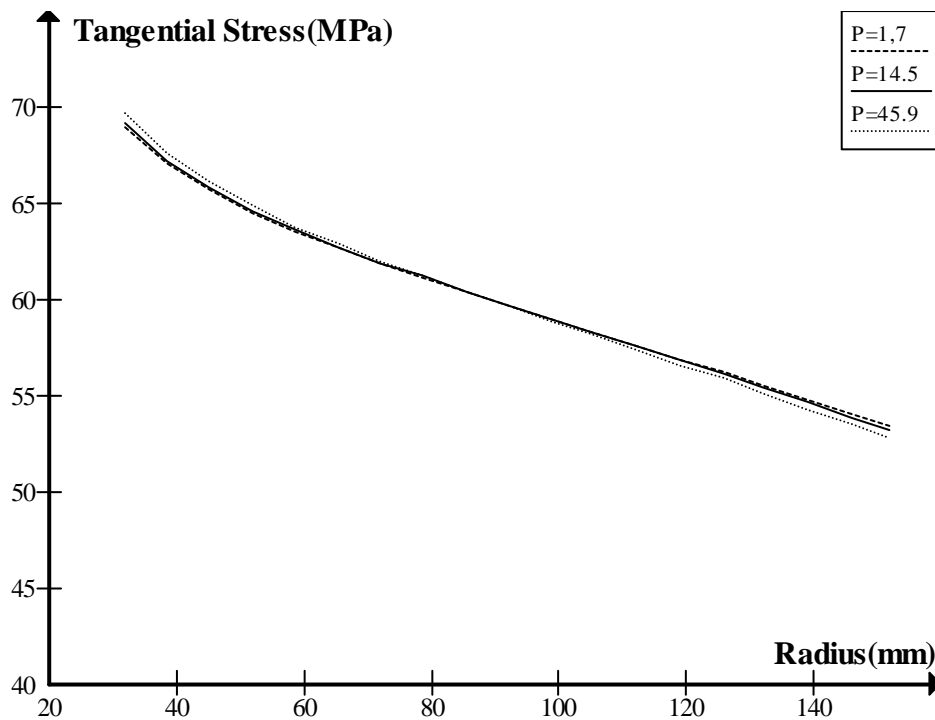


Fig 5.8: Effects of varying particle size of dispersoids (SiC_p) on tangential stress.

Fig 5.8 shows the creep response of the composite disc for varying particle size of the reinforcement for tangential stress. The values of the tangential stress decreasing continuously from inner to outer radius. Like radial stresses, tangential stresses also not too much affected by the particle size of reinforcement. The maximum variation observed in tangential as well as radial stress is approximately 1%.

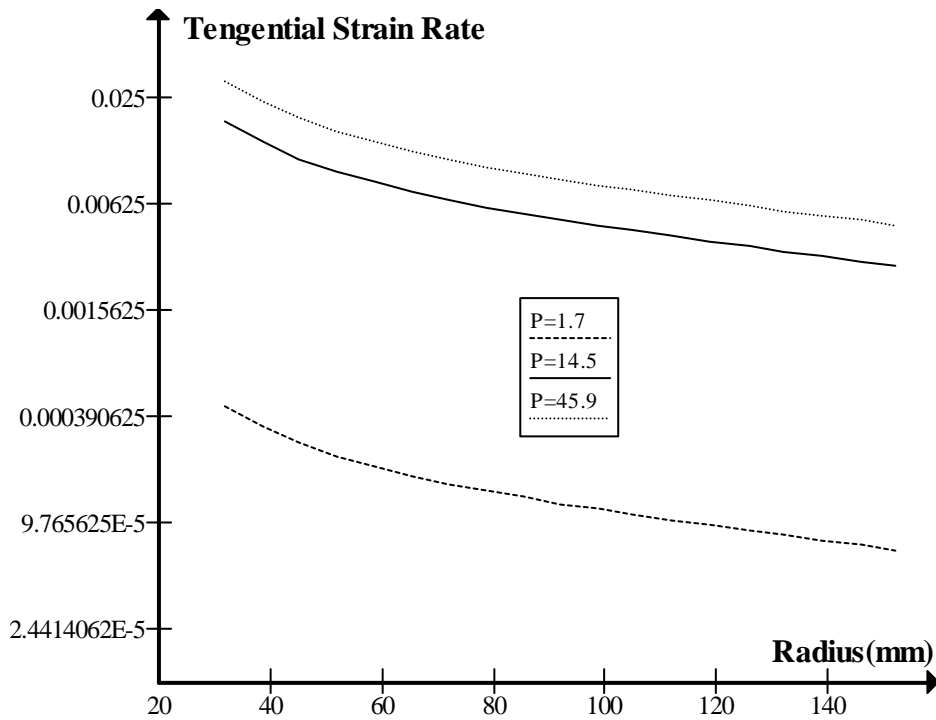


Fig 5.9: Effects of varying particle size of dispersoids (SiC_p) on tangential strain rate.

Fig. 5.9 shows the variation of tangential strain rate with radial distance. The change in particle size of the reinforcement affects the tangential strain rate quite significantly. It is estimated that the smaller size particles will be more in number for the any given volume fraction and are able to restrain creep flow more effectively. It is clear from the figure as the creep rate at any radius is reduced when the particle size decreases from 45.9 μm to 1.7 μm to a great extent.

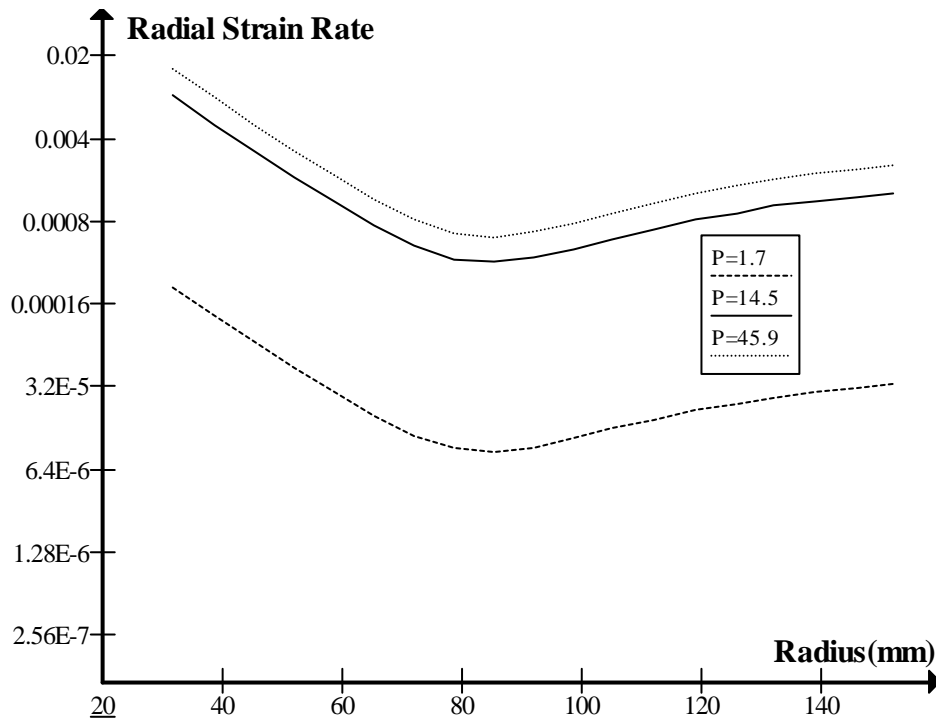


Fig 5.10: Effects of varying particle size of dispersoids (SiC_p) on radial strain rate:

Fig 5.10 shows the effect of particle size on radial strain rate. The radial strain rates decrease with radius up to a certain radius where it becomes minimum, beyond this value it increases slightly moving towards outer radius. Like the tangential strain rate, the radial strain rate is also significantly affected by the particle size of the reinforcement. The radial strain rate is also reduced when the particle size decreases from 45.9 μm to 1.7 μm .

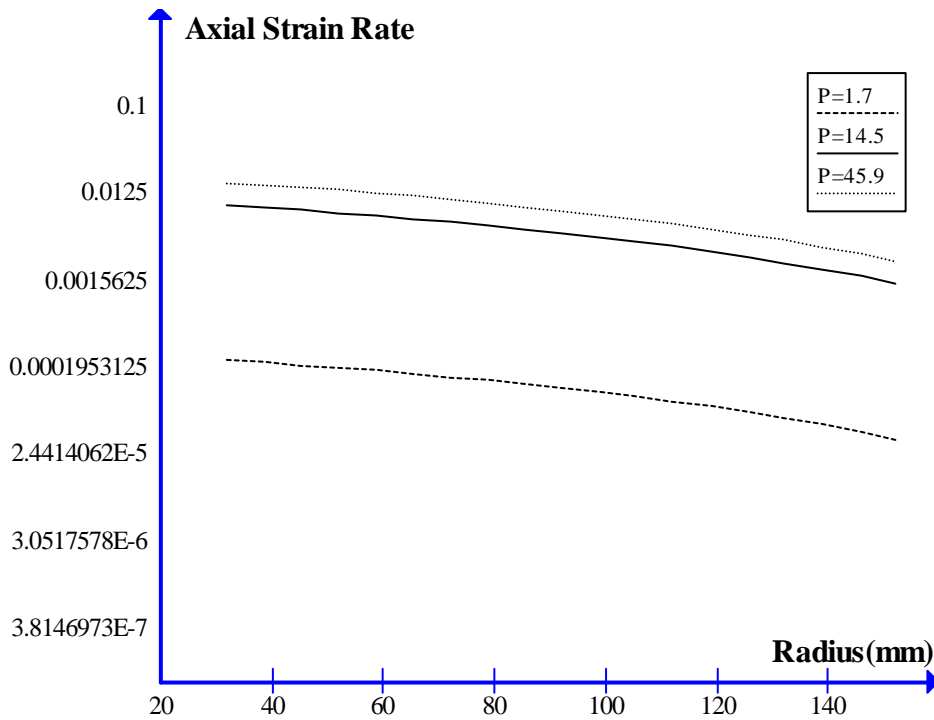


Fig 5.11: Effects of varying particle size of dispersoids (SiC_p) on axial strain rate.

Fig 5.11 shows the effect of particle size on axial strain rate. The axial strain rates decrease from inner to outer radius of the disc. Like the tangential strain rate and the radial strain rate, axial strain rate is also significantly affected by the particle size of the reinforcement. The axial strain rate is also reduced when the particle size decreases from 45.9 μm to 1.7 μm .

It can be clearly said that although creep stresses do not vary significantly with change in particle size but it has significant effect on strain rate.

CONCLUSIONS

Based on the obtained results and discussion presented in the previous chapter, the following conclusions are drawn:

1. The radial and tangential stresses in the disc could be significantly reduced by varying the disc profile. For the same disc volume and operating conditions, the tangential and radial stress in the disc having concave varying thickness are significantly lower than that observed in disc with either convex varying thickness or constant thickness.
2. The radial as well as tangential strain rates in the disc could be significantly reduced by employing disc with either concave or linear profile compared to uniform thickness disc. The disc having concave thickness profile has the lowest and more uniform distribution of strain rates.
3. The tangential as well as radial strain rate in the disc reduces significantly with reducing particle size but the radial and tangential stress is not too much affected by varying the particle size of reinforcement.

FUTURE SCOPE OF WORK

The study carried out in this thesis may be further extended in the following directions:

1. The study carried out in this thesis may be extended for disc operating under thermal gradients.
2. The effect of varying the disc profile may also be investigated for disc made of functionally graded material.
3. Analysis may be carried for disc having different boundary conditions.
4. Disc can also be considered which is subjected to internal pressure and/or external pressure.

REFERENCES

- [1] **Ahmet N. Eraslan**, “Elastic–Plastic Deformations of Rotating Variable Thickness Annular Disks With Free, Pressurized and Radially Constrained Boundary Conditions”, *International Journal of Mechanical Sciences*,(45), 643–667, **2003**.
- [2] **Ahmet N. ERASLAN and Yusuf Orcan**, “A Parametric Analysis of Rotating Variable Thickness Elastoplastic Annular Disks Subjected to Pressurized and Radially Constrained Boundary Conditions”, *International Journal of Engineering Sciences*, (28), 381 – 395, **2004**.
- [3] **Ashraf M.Zenukour**, “Analytical Solutions for Rotating Exponentially-Graded Annular Disc with Various Boundary Conditions”, *International Journal of Structural Stability and Dynamics*, (5), 557-577, **2005**.
- [4] **A.M. Afsar and J. Go**, “Finite Element Analysis of Thermoelastic Field in a Rotating FGM Circular Disk”, *International Journal of Applied Mathematical Modelling*, (34), 3309–3320, **2010**.
- [5] **Ashraf M. Zenkour, and Daoud S. Mashat**, “Stress Function of a Rotating Variable Thickness Annular Disk using Exact and Numerical Methods”, *International Journal of Engineering and Mathematics*, (3), 422-430, **2011**.
- [6] **Aidy Ali, M. Bayat, B. B. Sahari, M. Saleem and O. S. Zaroog**, “The Effect of Ceramic in Combinations of Two Sigmoid Functionally Graded Rotating Disks with Variable Thickness”, *International Journal of Mathematics*,7(25), 2174-2188, **2012**.
- [7] **C.O. Horgan and A.M. Chan**, “The Stress Response of Functionally Graded Isotropic Linearly Elastic Rotating Disks”, *Journal of Elasticity*, (55), 219–230, **1999**.

- [8] **D. Deepak, V.K Gupta, and A.K Dham**, “Impact of Stress Exponent on Steady State Creep in a Rotating Composite Disc”, *The Journal of Strain Analysis for Engineering Design*, (44),44-127, **2008**.
- [9] **D. Deepak, V. K. Gupta and A. K. Dham**, “Creep modeling in Functionally Graded Rotating Disc of Variable Thickness”, *Journal of Mechanical Science and Technology*, (11), 2221-2232, **2010**.
- [10] **Dharmpal Deepak, Vinay K. Gupta and Ashok K. Dham**, “Steady State Creep in a Rotating Composite Disc of Variable Thickness”, *International Journal of Mat. Research*, (6), 10, **2010**.
- [11] **Debabrata Das, Prasanta Sahoo and Kashinath Saha**, “Dynamic Analysis of Rotating Annular Disk of Variable Thickness under Uniform Axial Pressure”, *International Journal for Computational Methods in Engineering Science and Mechanics*, (13:1), 37-59, **2012**.
- [12] **G.J. Nie and R.C. Batra**, “Stress Analysis and Material Tailoring in Isotropic Linear Thermoelastic Incompressible Functionally Graded Rotating Disks of Variable Thickness”, *International Journal of Composite Structures* (92), 720–729, **2009**.
- [13] **Hamid Jahed and Jalal Bidabadi**, “An Axisymmetric Method of Creep Analysis for Primary and Secondary Creep”, *International Journal of Pressure Vessels and Piping*, (80), 597–606, **2003**.
- [14] **Hassani, M.H. Hojjati, E. Mahdavi, R.A. Alashti and G. Farrahi**, “Thermo Mechanical Analysis of Rotating Disks with Non-Uniform Thickness and Material Properties”, *International Journal of Pressure Vessels and Piping*, (98), 95-101, **2012**.
- [15] **Jyongsik Jang and Cholho Lee**, “Performance Improvement of GF/CF Functionally Gradient Hybrid Composite”, *International Journal of Material Properties*, (17), 383–394, **1997**.

- [16] **L.H. You, J.X. Wang and B.P. Tang**, “Deformations and Stresses in Annular Disks made of Functionally Graded Materials Subjected to Internal and/or External Pressure”, *International Journal of Meccanica*, (44), 283–292, **2008**.
- [17] **Mehdi Bayat, M. Saleem, B.B. Sahari, A.M.S. Hamouda and E. Mahdib**, “Analysis of Functionally Graded Rotating Disks with Variable Thickness”, *International Journal of Mechanics Research Communications*,(35), 283–309, **2007**.
- [18] **Mehdi Bayat, M. Saleem, B.B. Sahari, A.M.S. Hamouda and E. Mahdi**, “Mechanical and Thermal Stresses in a Functionally Graded Rotating Disk with Variable Thickness Due to Radially Symmetry Loads”, *International Journal of Pressure Vessels and Piping*, (86), 357–372, **2008**.
- [19] **M. Bayat, B.B. Sahari, M. Saleem, Aidy Ali and S.V. Wong**, “Bending Analysis of a Functionally Graded Rotating Disk Based on the First Order Shear Deformation Theory”, *International Journal of Applied Mathematical Modelling*, (33), 4215–4230, **2009**.
- [20] **Mehdi Bayat, B. B. Sahari, E M. Saleem, A. M. S. Hamouda and J. N. Reddy**, “Thermo Elastic Analysis of Functionally Graded Rotating Disks with Temperature-Dependent Material Properties: Uniform and Variable Thickness”, *Int J Mech Mater Des*,(5), 263–279, **2009**.
- [21] **N.J. LEE and J. JANG**, “Characterization of Functionally Gradient Epoxy/Carbon Fibre Composite Prepared under Centrifugal Force”, *International Journal of Material Science*, (32), 2013- 2020, **1997**.
- [22] **Pankaj Thakur, Singh S.B. and Jatinder Kaur**, “Thickness Variation Parameter in a Thin Rotating Disc by Finite Deformation”, *International Journal of Applied Mathematical Modelling*, (41), 96-102, **2013**.

- [23] **S.A. Hosseini Kordkheili and R. Naghdabadi**, “Thermoelastic Analysis of a Functionally Graded Rotating Disk”, *International Journal of Composite Structures*, (79), 508–516, **2006**.
- [24] **Shubhankar Bhowmick, Dipten Misra and Kashi Nath Saha**, “Variational Formulation Based Post-Elastic Analysis of Rotating Disks With Varying Thickness”, *International Conference on Mechanical Engineering*, (AM-07), 26-28, **2009**.
- [25] **Sanjeev Sharma, Manoj Sahni and Ravindra Kumar**, “Elastic-Plastic Analysis of a Thin Rotating Disk of Exponentially Variable Thickness with Inclusion”, *International Journal of Mathematics*, (9), 1109-2769, **2010**.
- [26] **Sanjeev Sharma, and Manoj Sahni**, “Elastic-Plastic Analysis for Finite Deformation of a Rotating Disk having Variable Thickness with Inclusion”, *World Academy of Science, Engineering and Technology*, (51), 456-465, **2011**.
- [27] **V.K. Gupta, S. B. Singh, H. N. Chandrawat and S. Ray**, “Steady State Creep and Material Parameters in a Rotating Disc of Al-SiC_p Composites”, *European Journal of Mechanics A/Solids*,(23) ,335-344, **2003**.
- [28] **V.K. Gupta, S.B. Singh, H.N. Chandrawat and S. Ray**, “Creep Behaviour of a Rotating Functionally Graded Composite Disc Operating under Thermal Gradient”, *International Journal of Metallurgical and Materials Transactions*, (35), 1381-1391, **2004**.
- [29] **Autar K. Kaw**, “Mechanics of Composites Materials”, *CRC Press Boca Raton, New York*, 2-18, **1997**.
- [30] **George E. Deiter**, “Mechanical Metallurgy”, *McGraw-Hill Book Company, Maryland*, **1928**.
- [31] www.share.pdfonline.com

[32] www.abdmatrix.com